NASA TECHNICAL NOTE

NASA TN D-5716

c. 1

NASA TN D-5716

ANALYSIS AND VERIFICATION OF A SPACECRAFT WIDE-ANGLE ATTITUDE-CONTROL SYSTEM

by Francis J. Moran and Bruce H. Dishman

Ames Research Center
Moffett Field, Calif.

NATIONAL AERONAUTICS AND SPACE ADMINISTRATION • WASHINGTON, D. C. • MARCH 1970

1. Report No. NASA TN D-5716	2. Government Accession No.	3. Recipient's Catalog No.
4. Title and Subtitle ANALYSIS AND VERIFICATION OF A SPACECRAFT WIDE-ANGLE ATTITUDE-CONTROL SYSTEM		5. Report Date March 1970
		6. Performing Organization Code
7. Author(s) Francis J. Moran and Bruce H. Dishman		8. Performing Organization Report No. A-2863
9. Performing Organization Name and Address NASA Ames Research Center Moffett Field, Calif., 94035		10. Work Unit No. 125-19-03-09-00-21
		11. Contract or Grant No.
12. Sponsoring Agency Name and Address National Aeronautics and Space Administration Washington, D. C., 20546		13. Type of Report and Period Covered TECHNICAL NOTE
		14. Sponsoring Agency Code

15. Supplementary Notes

16. Abstract

Attitude control to ensure stability of a spacecraft sluing through large angles was experimentally investigated. The investigation examined a control law synthesized from Euler's theorem on rotation, which states that any attitude change of a rigid body may be accomplished by a single rotation about the appropriate axis. A theoretical analysis showed that a system using the control law is globally stable.

The investigation was performed using an air-bearing table to simulate the spacecraft, two gimbaled star trackers as position sensors, rate gyroscopes to provide damping information, and reaction wheels as control torquers. Also a digital computer was used as a real-time controller to determine the desired axis of rotation from the star-tracker gimbal outputs and to generate simultaneous commands to all torquers so that the table would rotate about the desired axis.

17. Key Words Suggested by Author(s) Euler's theorem Inertially oriented attitude control	18. Distribution Statement Unclassified - Unlimited		
19. Security Classif. (of this report) Unclassified	20. Security Classif. (of this page) Unclassified	21. No. of Pages 44	22. Price* $3.00

*For sale by the Clearinghouse for Federal Scientific and Technical Information
Springfield, Virginia 22151
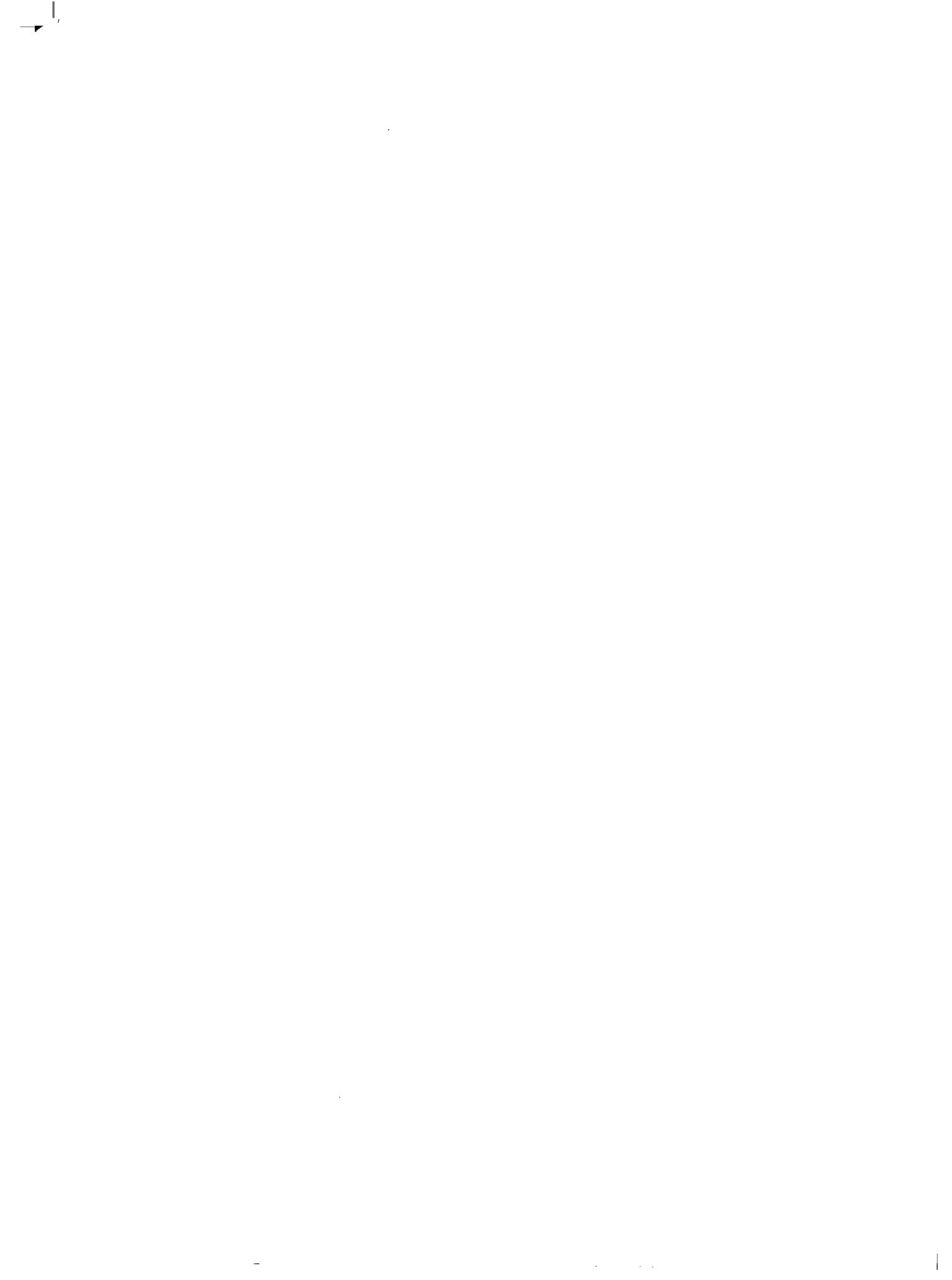
$\overline{a}_j$ vectors attached to the vehicle's marked axes defining the spacecraft coordinate system; $\overline{a}_1$, $\overline{a}_2$, and $\overline{a}_3$ define the roll, pitch, and yaw axes, respectively

$\overline{a}_j(0)$ initial orientation of the spacecraft coordinate system

A_{as} 3 × 3 direction cosine matrix defining the orientation of the spacecraft coordinate system $\overline{a}$ with respect to the inertial coordinate system $\overline{s}$

$\dot{A}_{as}$ time derivative of matrix A_{as}

$A_{as}(0)$ initial value of matrix A_{as}

A_{ds} 3 × 3 direction cosine matrix defining the orientation of the commanded spacecraft coordinate system $\overline{d}$ with respect to the inertial coordinate system $\overline{s}$

A_i, A_o inner and outer gimbal angles of star tracker 3

B_a 3 × 3 nonorthogonal matrix defining the orientation of the composite tracker coordinate system $\overline{T}$ with respect to the spacecraft coordinate system $\overline{a}$

B_s 3 × 3 nonorthogonal matrix defining the orientation of the composite tracker coordinate system $\overline{T}$ with respect to the inertial coordinate system $\overline{s}$

$\overline{c}$ unit eigenvector of the spacecraft-attitude-error matrix

c_j components of the eigenvector $\overline{c}$ in the body roll, pitch, and yaw axes, respectively

$c\theta$ cosine θ

$\overline{d}_j$ vectors defining the commanded position of the spacecraft coordinate system

$\overline{H}$ vector angular momentum of the system

I_{aj} moment of inertia of the spacecraft measured about the $\overline{a}_1$, $\overline{a}_2$, and $\overline{a}_3$ axes, respectively

I_{am} maximum value of I_{aj} (I_{a3} for this paper)

---

[1]All triads of vectors are orthonormal and form a right-handed set unless otherwise stated.

I_{wj} — moment of inertia of the roll, pitch, and yaw reaction wheels, respectively

k_{1j} — gain terms associated with the control law about the body roll, pitch, and yaw axes, respectively

k_2 — rate-gain term associated with the control law

K_i, K_o — inner and outer gimbal angles of star tracker 2

R — 3×3 direction cosine matrix defining the orientation of the spacecraft coordinate system $\bar{a}$ with respect to the commanded coordinate system $\bar{d}$ (error matrix)

$s\theta$ — sine θ

$\bar{s}_j$ — vectors defining the inertial coordinate system

$\bar{T}_j$ — composite tracker coordinate system; nonorthogonal triad of vectors forming a right-handed system; $\bar{T}_2$ and $\bar{T}_3$ are the lines of sight to stars 2 and 3, respectively; $\bar{T}_1 = \bar{T}_2 \times \bar{T}_3$

$\bar{T}_{2j}$ — vectors defining the orientation of star tracker 2

$\bar{T}_{3j}$ — vectors defining the orientation of star tracker 3

Z_j — control voltage to the motors of the spacecraft reaction wheels about the body's marked roll, pitch, and yaw axes

Z_m — maximum allowable value of voltage to reaction-wheel motor

Φ — angle of rotation about the desired Euler axis

Φ_s — magnitude of Φ at which Z_j saturates; for this investigation, $\Phi_s = 0.5°$

$\left.\begin{array}{l} \Phi_{large} \\ \\ \Phi_{small} \end{array}\right\}$ — $\left.\begin{array}{l} 0° \leq \Phi \leq 180° \\ \\ 0° \leq \Phi \leq 5° \end{array}\right\}$ Notation used only with strip chart recorder; the behavior of $\Phi \leq 5°$ is shown with a different recorder gain than $0° \leq \Phi \leq 180°$

ψ, ϕ, θ — yaw, roll, and pitch Euler angles defining the orientation of the air-bearing table; order of rotation is as shown

ω_{aj} — inertial angular rates of the body about the $\bar{a}_1$, $\bar{a}_2$, and $\bar{a}_3$ axes, respectively

ω_{am} — maximum component of body inertial rate

ω_{cj} — computed values of ω_{aj}; it refers to rates computed from the attitude matrix or from tachometers

ω_{wj} roll, pitch, and yaw reaction-wheel angular rates, respectively

$\omega_{wj}(0)$ initial speeds of three reaction wheels

Subscript

j   axis system components, $j = 1, 2, 3$

ANALYSIS AND VERIFICATION OF A SPACECRAFT

WIDE-ANGLE ATTITUDE-CONTROL SYSTEM

Francis J. Moran and Bruce H. Dishman

Ames Research Center

SUMMARY

Attitude control to ensure stability of a spacecraft sluing through large angles was experimentally investigated. The investigation examined a control law synthesized from Euler's theorem on rotation, which states that any attitude change of a rigid body may be accomplished by a simple rotation about an appropriate axis. The theoretical analysis showed that a system using the control law is globally stable.

The purpose of this investigation was to verify by means of an air-bearing table simulation the behavior of a system using the control law. It also was desired to compare the operation of the control law when vehicle rate information was obtained from (1) rate gyroscopes, (2) the spacecraft-attitude direction cosine matrix, and (3) tachometers mounted on the reaction wheels. The system using rate-gyro information was tested with and without initial angular momentum; the other two methods were tested only with zero initial momentum.

The experimental apparatus used in this analysis was an air-bearing table representing the spacecraft, three reaction wheels for control, three rate gyros for vehicle rate information, and two gimbaled star trackers for position information. An online digital computer performed as a real-time controller. The computer calculated the desired axis of rotation from the star-tracker information and generated simultaneous commands to the three torquers. The three control signals were converted to analog form and transmitted to the reaction-wheel torquers.

The results of the simulation show that the system using the control law performed as predicted by theory. The air-bearing table rotated about the desired axis while sluing through angles of 55° in yaw and 10° in pitch and roll. The combined steady-state error about all three axes was 0.1°, which represents the sensitivity limit of the attitude sensors.

INTRODUCTION

The need for a system that ensures stability while controlling the rotational position of a rigid body sluing through large angles is encountered in a program such as the Orbiting Astronomical Observatory (OAO). The problem is to point a telescope, rigidly attached to the spacecraft, in any

direction dictated by a ground-based observer. The present OAO program accomplishes wide-angle sluing by commanding the vehicle to complete a sequence of open-loop, single-axis maneuvers (ref. 1). The slue-control system reorients the vehicle to within the limits of the coarse control system. The coarse control system then stabilizes the satellite by resolving the star-tracker gimbal angles into the proper components to drive the vehicle so that the target star is within the field of view of the telescopes. Reference 2 describes another attitude-control system that uses the star-tracker gimbal-angle information to stabilize the satellite.

The purpose of this investigation was to simulate and verify a control law that could be used for both stabilization and reorientation. The control law was synthesized from Euler's theorem on rotation, which states that any attitude change of a rigid body may be accomplished by a single rotation about an appropriate axis. It also was desired to compare the behavior of the system when the rate information required by the control law was obtained from gyros, the attitude direction cosine matrix, and tachometers mounted on the reaction wheels.

The control-system simulation was performed on a three-degrees-of-freedom air-bearing table. The experimental apparatus used with the table consisted of two gimbaled star trackers as position sensors, reaction wheels as torquers, rate gyros for damping, and a digital computer as an online controller.

The report first describes the experimental apparatus used to verify the control law. The attitude-error matrix equation is then developed followed by a brief review of the attitude control law. Then the methods of deriving inertial angular body rates from the vehicle-attitude matrix and the reaction-wheel tachometers are developed. Finally, the test procedures and results describing the performance of a system using the control law are presented.

EXPERIMENTAL APPARATUS

The attitude-control system was mechanized on the Ames satellite attitude-control simulator (fig. 1), which includes an air-bearing table in a vacuum chamber that can be evacuated to a pressure of 1 mm Hg. (The chamber was never evacuated during the simulation.) Both the chamber and the air-bearing table are mounted on a seismic foundation to isolate the table from ground disturbances. The air-bearing table configuration and the control-system package used for this analysis is shown in figure 2. The complete package weighed 1800 lb; its inertia was 180 slug-ft^2 about the yaw axis and 145 slug-ft^2 about the pitch and roll axes. The air-bearing table has unlimited freedom of motion about the yaw axis and is limited to ±29° about the pitch and roll axes. (The simulator is described in greater detail in the appendix.)

The attitude of the table is controlled by three inertia wheels located along the control axes of the table (fig. 2). The inertia wheels are driven by dc motors with a stall torque of 15 in.-oz. The motor and reaction wheel

combination has a time constant of 35 sec and a maximum speed of 3000 rpm. The inertia of the wheels was 0.014 slug-ft^2. The angular velocity of the reaction wheel was available from a tachometer.

The attitude information used to generate the control signals was derived from two gimbaled star trackers, which are positioned on the table so that their outer gimbal axes are parallel and aligned with the table's roll axis. The trackers have angular freedom of ±50° about both the inner and outer gimbal axes. The angular position of the gimbals was determined by measuring the output of a resolver, which has an accuracy of ±5.0 min of arc. The star trackers have a maximum sluing rate of 0.75° per sec.

The trackers point at simulated stars located within the air-bearing-table chamber. The star simulators have a clear aperture of 12 in. and provide a star beam collimated to within ±5.0 arc sec relative to the optical axis. The star can be adjusted from -2.0 to +6.5 apparent star magnitude.

The output from the two star trackers, the three rate gyros, and the three tachometers on the table was sent in analog form to a digital computer. This computer acts as a real-time controller for the air-bearing table in that it accepts the basic analog signals, converts them to digital data, and performs the necessary matrix operations to generate the specified control law. The use of Fortran, facilitated computer changes in the control law. The system program was cycled through the computer at a frequency of about 30 Hz. The control signals generated by the computer were transmitted in analog form to the reaction wheels.

DEVELOPMENT OF THE ATTITUDE-ERROR MATRIX EQUATION

The position information required by the control law makes it necessary to derive a measure of the error in attitude. The first section describes the development of the attitude error matrix. The second section describes the determination of the satellite's attitude from the star tracker information which is necessary to calculate the error matrix.

Development of the Error Matrix

The commanded orientation of the spacecraft with respect to the inertial coordinate system (fig. 3) is given by:[2]

$$\begin{pmatrix} \overline{d}_1 \\ \overline{d}_2 \\ \overline{d}_3 \end{pmatrix} = A_{ds} \begin{pmatrix} \overline{s}_1 \\ \overline{s}_2 \\ \overline{s}_3 \end{pmatrix} \tag{1}$$

---

[2]Figure 3 shows the star-tracker inner-gimbal angles at zero. Thus, vectors $\overline{T}_{21}$ and $\overline{T}_{31}$ are oriented along the two outer gimbal axes. Vectors $\overline{d}_2$ and $\overline{d}_3$ are also shown lying in the $\overline{a}_1$ and $\overline{a}_2$ plane. This arrangement is for convenience in drawing and does not represent the general case.

The present position of the vehicle with respect to the inertial coordinate system is given by:

$$\begin{pmatrix} \overline{a}_1 \\ \overline{a}_2 \\ \overline{a}_3 \end{pmatrix} = A_{as} \begin{pmatrix} \overline{s}_1 \\ \overline{s}_2 \\ \overline{s}_3 \end{pmatrix} \qquad (2)$$

From equations (1) and (2) and the fact that A_{ds} is an orthogonal matrix, it follows that the actual position of the vehicle with respect to the desired position is given by:

$$\begin{pmatrix} \overline{a}_1 \\ \overline{a}_2 \\ \overline{a}_3 \end{pmatrix} = A_{as} A_{ds}^T \begin{pmatrix} \overline{d}_1 \\ \overline{d}_2 \\ \overline{d}_3 \end{pmatrix} \qquad (3)$$

Equation (3) shows that the vehicle attains the desired attitude when the matrix product $A_{as} A_{ds}^T$ forms an identity matrix. This product is defined as the error matrix R:

$$R = A_{as} A_{ds}^T \qquad (4)$$

When the vehicle $\overline{a}$ is in its desired orientation $\overline{d}$, then $R = I$. Therefore, the deviation of R from I is a measure of the error in the attitude of the spacecraft. The control law information was extracted from this matrix.

Determination of Spacecraft Attitude

The attitude matrix A_{as} must be determined as a basis for calculating R; the matrix A_{ds} is given. The attitude of the spacecraft can be defined with respect to the lines of sight to two stars. If it is assumed that the tracker perfectly tracks the star, then the lines of sight to the stars coincide with the tracker's optical axes. The attitude of the spacecraft can now be defined with respect to the optical axes of the two trackers. For example, the relationships between the star-tracker coordinate system and the spacecraft are

$$\begin{pmatrix} \overline{T}_{21} \\ \overline{T}_{22} \\ \overline{T}_{23} \end{pmatrix} = X(K_i)V(K_o)Y(1) \begin{pmatrix} \overline{a}_1 \\ \overline{a}_2 \\ \overline{a}_3 \end{pmatrix} \qquad (5)$$

and

$$\begin{pmatrix} \overline{T}_{31} \\ \overline{T}_{32} \\ \overline{T}_{33} \end{pmatrix} = W(A_i)V(A_o)Y(2) \begin{pmatrix} \overline{a}_1 \\ \overline{a}_2 \\ \overline{a}_3 \end{pmatrix} \qquad (6)$$

4

where

$$X(K_i) = \begin{pmatrix} cK_i & sK_i & 0 \\ -sK_i & cK_i & 0 \\ 0 & 0 & 1 \end{pmatrix}$$

$$V(K_o) = \begin{pmatrix} 1 & 0 & 0 \\ 0 & cK_o & sK_o \\ 0 & -sK_o & cK_o \end{pmatrix}$$

$$Y(1) = \begin{pmatrix} 1 & 0 & 0 \\ 0 & 1 & 0 \\ 0 & 0 & 1 \end{pmatrix}$$

$$W(A_i) = \begin{pmatrix} cA_i & 0 & -sA_i \\ 0 & 1 & 0 \\ sA_i & 0 & cA_i \end{pmatrix}$$

$$V(A_o) = \begin{pmatrix} 1 & 0 & 0 \\ 0 & cA_o & sA_o \\ 0 & -sA_o & cA_o \end{pmatrix}$$

$$Y(2) = \begin{pmatrix} 1 & 0 & 0 \\ 0 & -1 & 0 \\ 0 & 0 & -1 \end{pmatrix}$$

Let $\overline{T}_2$ and $\overline{T}_3$ be unit vectors in the direction of the lines of sight of stars 2 and 3, respectively. Then

$$\left. \begin{array}{l} \overline{T}_2 \equiv \overline{T}_{22} \\ \overline{T}_3 \equiv \overline{T}_{33} \end{array} \right\} \tag{7}$$

A third vector is defined as

$$\overline{T}_1 = \overline{T}_2 \times \overline{T}_3 \tag{8}$$

where $\overline{T}_1$ is not, in general, a unit vector. The $\overline{T}_1, \overline{T}_2, \overline{T}_3$ coordinate system, called the tracker coordinate system, usually is nonorthogonal. The relationship between the tracker coordinate system and the spacecraft coordinate system is

$$\begin{pmatrix} \overline{T}_1 \\ \overline{T}_2 \\ \overline{T}_3 \end{pmatrix} = B_a \begin{pmatrix} \overline{a}_1 \\ \overline{a}_2 \\ \overline{a}_3 \end{pmatrix} \tag{9}$$

5

In a real application, the location of the stars with respect to inertial space would be obtained from some astronomical data source. The location of the simulated stars with respect to the inertial space used for the simulator is determined from the star-tracker gimbal angles and the table Euler angle measurements. For example,

$$\begin{pmatrix} \overline{T}_{21} \\ \overline{T}_{22} \\ \overline{T}_{23} \end{pmatrix} = X(K_i)V(K_o)Y(1)A_{as}(K) \begin{pmatrix} \overline{s}_1 \\ \overline{s}_2 \\ \overline{s}_3 \end{pmatrix} \tag{10}$$

and

$$\begin{pmatrix} \overline{T}_{31} \\ \overline{T}_{32} \\ \overline{T}_{33} \end{pmatrix} = W(A_i)V(A_o)Y(2)A_{as}(K) \begin{pmatrix} \overline{s}_1 \\ \overline{s}_2 \\ \overline{s}_3 \end{pmatrix} \tag{11}$$

where

$$A_{as}(K) = \begin{pmatrix} c\theta K & 0 & -s\theta K \\ 0 & 1 & 0 \\ s\theta K & 0 & c\theta K \end{pmatrix} \begin{pmatrix} 1 & 0 & 0 \\ 0 & c\phi K & s\phi K \\ 0 & -s\phi K & c\phi K \end{pmatrix} \begin{pmatrix} c\psi K & s\psi K & 0 \\ -s\psi K & c\psi K & 0 \\ 0 & 0 & 1 \end{pmatrix} \tag{12}$$

Equation (12) is calculated for known table Euler angles and is used in equations (10) and (11) in conjunction with known tracker gimbal angles. Since $\overline{T}_2 \equiv \overline{T}_{22}$ and $\overline{T}_3 \equiv \overline{T}_{33}$, the position of the tracker coordinate system relative to inertial space is

$$\begin{pmatrix} \overline{T}_1 \\ \overline{T}_2 \\ \overline{T}_3 \end{pmatrix} = B_s \begin{pmatrix} \overline{s}_1 \\ \overline{s}_2 \\ \overline{s}_3 \end{pmatrix} \tag{13}$$

The tracker gimbal angle and table Euler angle measurements are then used to calculate B_s. The B_s matrix locates the simulated stars with respect to the inertial frame. If the right side of equations (9) and (13) are equated, one obtains

$$\begin{pmatrix} \overline{s}_1 \\ \overline{s}_2 \\ \overline{s}_3 \end{pmatrix} = B_s^{-1}B_a \begin{pmatrix} \overline{a}_1 \\ \overline{a}_2 \\ \overline{a}_3 \end{pmatrix} \tag{14}$$

Comparing equations (14) and (2), one can write

$$A_{as} = (B_s^{-1}B_a)^T \tag{15}$$

Then the error matrix R, defined in equation (4), can be written as

$$R = (B_s^{-1}B_a)^T A_{ds}^T \tag{16}$$

6

In a space application, the matrix B_s, which defines the orientation of the composite tracker coordinate system when locked on the selected guide stars to the inertial coordinate system, would be obtained directly from astronomical data.

THE ATTITUDE CONTROL LAW

The control law was synthesized from Euler's theorem on rotation (ref. 3), which states that any attitude change of a rigid body can be accomplished by a single rotation about an appropriate axis. The axis of rotation is defined by the eigenvector $\bar{c}$ of the error matrix R. The angle of rotation about $\bar{c}$ to make the body axes coincident with the desired axis is defined as Φ. The command to the reaction-wheel motors to rotate the spacecraft through an angle Φ about the eigenvector $\bar{c}$ is

$$Z_j = -k_{1j}[sat(\Phi, \Phi_s)c_j + k_2\omega_{aj}] \qquad j = 1, 2, 3 \qquad (17)$$

where Z_j is the control voltage to the jth reaction wheel, ω_{aj} is the body angular rate about the jth marked body axis, and k_{1j} and k_2 are constants. The first term in the brackets represents the position information and is obtained from the error matrix R determined in the previous section. The term $sat(\Phi, \Phi_s)$ is

$$sat(\Phi, \Phi_s) = \begin{cases} 1 & \text{for} \quad \Phi \geq \Phi_s \\ \dfrac{\Phi}{\Phi_s} & \text{for} \quad \Phi < \Phi_s \end{cases}$$

where the magnitude of rotation Φ is

$$\Phi = \cos^{-1} \frac{1}{2}(R_{11} + R_{22} + R_{33} - 1) \qquad (18)$$

and

$$\Phi_s = 0.5°$$

The direction of rotation is given by the components of the eigenvector $\bar{c}$ which are

$$c_1 = \frac{1}{2} \frac{R_{23} - R_{32}}{\sin \Phi}$$

$$c_2 = \frac{1}{2} \frac{R_{31} - R_{13}}{\sin \Phi}$$

$$c_3 = \frac{1}{2} \frac{R_{12} - R_{21}}{\sin \Phi}$$

The R_{ij} terms refer to the off-diagonal components of the error matrix R.

The control law can be approximated when the error in attitude is small. The approximation is desired because the eigenvector orientation is not defined when $\Phi = 0$. Thus, the components of the eigenvector become noisy when $\Phi \leq \Phi_s$. If $\Phi \leq \Phi_s$, then $\Phi \approx \sin \Phi$. The control law (eq. (17)) can then be written as

$$z_j = -k_{1j} \left(\frac{q_j}{\Phi_s} + k_2 \omega_{aj} \right) \qquad j = 1, 2, 3 \qquad (19)$$

where q_j are

$$q_1 = \frac{1}{2} (R_{23} - R_{32})$$

$$q_2 = \frac{1}{2} (R_{31} - R_{13})$$

$$q_3 = \frac{1}{2} (R_{12} - R_{21})$$

The control law given by equation (19) is independent of the components of the eigenvector. A block diagram of the control law computation is shown in figure 4.

The rate information required by the control law (eqs. (17) and (19)) was obtained by three different methods: (1) directly from the rate gyroscopes, considered the basic mode of operation; (2) from A_{as} matrix computations; and (3) from the reaction-wheel tachometer measurements. Methods (2) and (3) are considered backup systems to the gyroscopes.

The body rate is derived from the A_{as} matrix according to the relationship

$$\dot{A}_{as} = s(\omega_a) A_{as} \qquad (20)$$

where

$$s(\omega_a) = \begin{pmatrix} 0 & \omega_{a3} & -\omega_{a2} \\ -\omega_{a3} & 0 & \omega_{a1} \\ \omega_{a2} & -\omega_{a1} & 0 \end{pmatrix} \qquad (21)$$

and $\dot{A}_{as}$ may be evaluated from

$$\dot{A}_{as} = \frac{A_{as}(n + 1) - A_{as}(n)}{T} \qquad (22)$$

8

which represents the discrete form of the time derivative of A_{as}; $A_{as}(n)$ and $A_{as}(n + 1)$ are values of the nine components of the A_{as} matrix at the beginning and end of a time interval specified by T. The matrix equation then takes the form:

$$
\begin{pmatrix} 0 & \omega_{a3} & -\omega_{a2} \\ -\omega_{a3} & 0 & \omega_{a1} \\ \omega_{a2} & -\omega_{a1} & 0 \end{pmatrix} = \left[\frac{A_{as}(n + 1) - A_{as}(n)}{T} \right] A_{as}^T(n) \tag{23}
$$

If $B = A_{as}(n + 1)A_{as}^T(n)/T$, then the components of the body rates are

$$
\left.\begin{aligned}
\omega_{c1} &= \frac{B_{23} - B_{32}}{2} \\[2mm]
\omega_{c2} &= \frac{B_{31} - B_{13}}{2} \\[2mm]
\omega_{c3} &= \frac{B_{12} - B_{21}}{2}
\end{aligned}\right\} \tag{24}
$$

where the notation ω_c, substituted for ω_a, indicates a computed value. The rates are obtained by summing and averaging the two solutions available for each rate component from equation (23).

To compute the body rates from reaction-wheel-tachometer information, two assumptions must be made: (1) the system is initially stabilized so that all the system momentum is stored in the reaction wheels; and (2) the system is conservative - that is, the external torques are zero. The total system momentum at any time is

$$
\overline{H} = (I_{a1}\omega_{a1} + I_{w1}\omega_{w1})\overline{a}_1 + (I_{a2}\omega_{a2} + I_{w2}\omega_{w2})\overline{a}_2 + (I_{a3}\omega_{a3} + I_{w3}\omega_{w3})\overline{a}_3 \tag{25}
$$

Since the total initial system momentum is stored in the motors, one can write

$$
\overline{H} = I_{w1}\omega_{w1}(0)\overline{a}_1(0) + I_{w2}\omega_{w2}(0)\overline{a}_2(0) + I_{w3}\omega_{w3}(0)\overline{a}_3(0) \tag{26}
$$

The starting position of the body $\overline{a}_i(0)$ can be expressed in terms of the body position at any time $\overline{a}_i$ as

$$
\begin{pmatrix} \overline{a}_1(0) \\ \overline{a}_2(0) \\ \overline{a}_3(0) \end{pmatrix} = A_{as}(0) \begin{pmatrix} \overline{s}_1 \\ \overline{s}_2 \\ \overline{s}_3 \end{pmatrix} = A_{as}(0)A_{as}^T(t) \begin{pmatrix} \overline{a}_1 \\ \overline{a}_2 \\ \overline{a}_3 \end{pmatrix} \tag{27}
$$

Substituting equation (27) into equation (26) and then equating equations (25) and (26), one obtains

9

$$MP \begin{pmatrix} \overline{a}_1 \\ \overline{a}_2 \\ \overline{a}_3 \end{pmatrix} = N \begin{pmatrix} \overline{a}_1 \\ \overline{a}_2 \\ \overline{a}_3 \end{pmatrix}$$

where M and N are 1×3 row ratrices whose components are given as

$$\left. \begin{array}{l} M_j = I_{wj}\omega_{wj}(0) \\[2mm] N_j = I_{aj}\omega_{aj} + I_{wj}\omega_{wj} \end{array} \right\} \quad j = 1, 2, 3$$

and

$$P = A_{as}(0)A_{as}^{T}(t)$$

Solving for ω_{aj}, and denoting it by ω_{cj} to indicate a computed value, yields

$$\omega_{cj} = \frac{\displaystyle\sum_{l=1}^{3} M_l P_{lj} - I_{wj}\omega_{wj}}{I_{aj}} \quad j = 1, 2, 3 \tag{28}$$

TEST PROCEDURES AND RESULTS

The theoretical study (ref. 3) shows that a vehicle sluing under the influence of the previously given control law will move about the eigenvector of the R matrix. The time history of the angle Φ and the components of the eigenvector $\overline{c}$ are a measure of the control-system performance. If the total system momentum remains zero, the time history of the $\overline{c}$ components should be a constant value and the angle Φ should be a decreasing function of constant slope. The final value of Φ gives the system-pointing error.

The results of the simulation are summarized in figures 5 through 11. The results were output from the digital computer, through the digital analog converters to a strip chart recorder. Data were obtained once every computation cycle (35 msec). A line printer coupled directly to the digital computer provided numerical values for the data. A printout was made at the beginning and end of each slue. The numerical values are shown in parenthesis on the figures. The parameters displayed in the figures include the angle Φ, the eigenvector components c_j, the control voltages Z_j, and the body rates ω_{aj}. Since system-pointing accuracy as well as the wide-angle sluing characteristics were of interest, the level of control saturation was set at $\Phi_s = 0.5°$. The magnitude of k_{1j} was determined for each axis from the relationship

$$k_{1j} = \frac{Z_m I_{aj}}{I_{am}} \quad j = 1, 2, 3 \tag{29}$$

The gain factor k_2, which is the same for all three axes, is

$$k_2 = \frac{1}{\omega_{am}}$$

where ω_{am} was set equal to 0.4° per sec; that is, $k_2 = 2.5$.

Rate Gyroscopes

Figure 5 shows the response of the system when rate gyroscopes are used for damping. The table is positioned initially at Euler angles of -4.78° in roll, -5.74° in pitch, and 74.28° in yaw, and is commanded to slue to +5.0°, +5.0°, +20.0°. The direction between the eigenvector and the respective body axes is given by the inverse cosine of each $\overline{c}$ component. For this run, the initial orientation of the eigenvector with respect to the roll, pitch, and yaw axes is 81°, 79°55', and 13°25', respectively. As expected, the major component of the command is about the yaw axis. The time history of the eigenvector components shows that they remain nearly constant during the slue until $\Phi = 0.5°$. When $\Phi \leq \Phi_s$, the approximate control law, which is independent of $\overline{c}$, is used, and the eigenvector components vary rapidly as indicated by their traces in the figure.

The initial and commanded angles result in an angle $\Phi = 55.94°$. The time history of the angle Φ indicates that it decreases with a constant negative slope as predicted by the theory. The recorder sensitivity of Φ is increased when $\Phi \leq 5.0°$ to show the performance of the system near the target point. (The computer was programmed such that Φ small was zero until $\Phi = 5.0°$.) The trace of Φ shows that the system has two overshoots and settles to within 0.12° of the commanded value. As indicated by the Euler angles, the corresponding pointing error about each control axis is (0.02°, 0.08°, 0.02°).

From the time histories of the control voltages Z_j and the body rates ω_{aj}, it is observed that the voltage about the axis with a maximum error initially saturates and then decreases to a level necessary to maintain the maximum desired rate (ω_{am_d}). In this case, the yaw axis has the maximum error. The average control voltages about the roll and pitch axes are proportionally lower as determined by the values of the $\overline{c}$ components.

The behavior of the system using gyro damping to a sequence of commands is shown in figure 6. This sequence is mechanized by commanding the system to one position, letting it stabilize at this position, then commanding it to the second position, etc. The sequence of commands shows the behavior of the system in a scanning-type operation. Initially, the table's angular position is (0.34°, 0.39°, 54.60°) and is commanded to (-5°, -5°, +20°). For this command, the major control torque is about the yaw axis. The behavior of c_j and Φ is quite similar to the run discussed in figure 5. There is no momentum buildup during this phase of the run.

The second sequence commands the table to (+5°, +5°, +20°). During this maneuver, the control torques are entirely about the pitch and yaw axes, and

the eigenvector components vary slightly as a result of undesirable torques causing increased system momentum. At t = 178 sec the system is commanded to (-10°, -5°, +54°). During this maneuver the $\bar{\tau}$ components vary considerably because of the buildup of momentum. The initial system momentum and undesirable external torques cause the eigenvector orientation to change 17° between t = 183 sec and t = 260 sec. Nevertheless, the angle approaches zero in a nearly linear manner, and the system stabilizes with an error of 0.10°. The final command is (0°, 0°, 54°); the system stabilizes to within 0.10° of this position as indicated by the final value of Φ.

Rate From the A_{as} Matrix

Figures 7 and 8 show system response when rate damping information is derived from the A_{as} matrix. The procedure used is essentially a time differentiation that tends to amplify the system noise to an extent, in fact, that it completely masks the rate signal. To reduce the noise, the A_{as} matrix is averaged over 100 msec. The averaging process acts as a filter but does not introduce enough lag to affect the stability of the system. A comparison of the derived rate ω_{cj} and the rate from the gyroscope ω_{aj} shows that the derived rate, even when averaged, is more noisy.

The eigenvector components of the system using the derived rate show more variation than those of the system using the gyros (figs. 7 and 8). For example, the angle between the eigenvector at t = 0 and t = 125 sec was computed as 20°. However, both the transient and steady-state responses of the system are still quite acceptable.

Rate From the Reaction-Wheel Tachometers

Figure 9 shows control system damping in which the body rate information is computed from dc tachometers attached to the reaction wheels. Computations assumed zero external torques. However, the system is subjected to disturbance torques that cause variations in system momentum. At the initial and final positions, the system momentum is in the reaction wheels: the initial wheel speeds are zero, but the final wheel speeds are nonzero. The final body rate computed from the tachometer measurements, therefore, is nonzero and disagrees with the gyro information. The error in the rate signal can be observed by comparing the body rate signals derived from the tachometers to the gyro measurements on figure 9. At time t = 120 sec, the pitch-rate signal computed from the tachometer is of opposite sign from the true body-rate measurements. The final rate error is mainly in the pitch axis. From the data obtained, this system clearly has the worst response of the three tested, because the initial momentum vector changes as the system is subjected to disturbance torques. Since the computation is based on the system's initial momentum, any momentum change causes an error in the computed rate signal. The rate signal error caused the system to develop an additional position error as indicated by the Φ trace.

The increased steady-state error can be eliminated through updating the system momentum at the end of the maneuver. For example, assume the system

12

begins the maneuver with zero momentum and stabilizes with nonzero momentum. After the system stabilizes, one can calculate, by means of equation (26), the system momentum. The derived body rate can then be calculated in the prescribed manner. The effect of updating the system momentum is to eliminate the error in the derived body rate caused by the external torques. The results of this procedure are shown in figure 10. The new system momentum and the derived rates are recalculated at t = 217 sec. Note that the error in the derived body rates is reduced, and that the pointing error is reduced from 0.38° to 0.15°.

Nonzero Initial Momentum With Rate Gyroscopes

Figure 11 shows the effect of nonzero initial momentum on the behavior of the control system using rate gyros for damping. The tachometer traces show that the initial rates of the roll, pitch, and yaw reaction wheels were 1600, 1150, and 1050 rpm, respectively. The final wheel velocities were very close to these initial values, which implies a low-magnitude disturbance torque. During the run the c_j vary as would be expected since the momentum vector of the system is varying. The traces of the motor control voltages show the offset necessary to maintain the wheels spinning at the initial rate. Therefore, the system performance does not deteriorate significantly when the initial system momentum is nonzero. Furthermore the system is well behaved and has a pointing error of 0.12°.

CONCLUDING REMARKS

The results of the simulation show that the wide-angle attitude-control system based on Euler's theorem on rotation performs as predicted by the theoretical analysis. The angular motion is about the Euler rotation axis rather than about three axes separately. The system has proven global stability, and the angular rotation of the vehicle is well behaved and predictable during a slue.

The best method for obtaining rate information for the control law is the rate gyroscope. External torques or initial momentum that causes a variation in the eigenvector during the run does not cause a significant decrease in system performance. Inertial body rates also can be determined indirectly, which obviates a flight abort in case of rate gyroscope failure. The inertial body rates could be computed from either the reaction-wheel tachometer measurements or from the spacecraft-attitude matrix (A_{as}). The rates computed from the tachometer measurements are less noisy than the rates obtained from the attitude matrix. However, for the tachometer system, a variation in system momentum causes an increase in the steady-state pointing error, which can be decreased by updating the system momentum vector when the system reaches steady state. The performance of the system using the rates derived from the attitude matrix is not affected by varying system momentum.

The type of control system shown in this mechanization could be used very effectively on a vehicle such as the OAO, where the ability to command the spacecraft through large angles is desired.

Ames Research Center
    National Aeronautics and Space Administration
        Moffett Field, California, 94035, November 25, 1969

APPENDIX

DESCRIPTION OF SATELLITE ATTITUDE-CONTROL SIMULATOR

The attitude-control system of this report was mechanized on the Ames Satellite Attitude-Control Simulator (fig. 1). The air-bearing table is contained in a spherical chamber, which can be evacuated to a pressure of 1 mm Hg. The chamber and air-bearing-table assembly are supported on a seismic foundation.

The table rests on a 7-in.-diameter stainless steel ball supported by a cushion of air injected into a mating socket. The gap between the ball and the socket is 150 μin. Air is injected into the socket at a pressure of 70 psia, and is bled off from the socket and routed to control jets located on the three axes of the table. With these jets and the control console associated with the table, it is possible to control the position of the table independent of the control system package under test. It is possible to add inertia cones to the basic table and raise the inertia about the yaw axis to 750 slug-ft^2 and about the pitch and roll axes to 400 slug-ft^2.

Communications with the table and power to the table are transmitted via a mercury pool and slip ring assembly. From the table, signals pass through individual pins arranged in a circle and located on the table. The pins project into individual pools of mercury located on a following gimbal system. (The following gimbal system tracks the table by utilizing a three-axis, autocollimating error-detection system.) From the base of the mercury pools, the signals then pass through a slip-ring assembly, located on the yaw gimbal, which allows unlimited yaw motion. This technique of getting data on and off the table eliminates the disturbance torques that would be caused by hanging wires from above the table and the complexity of telemetering the data.

Also connected to the following gimbal system are position and rate encoders that give the table Euler angles and rates in a natural binary form at the control console. This information is then converted into a visual readout.

REFERENCES

1. Zetkov, George; and Fleisig, Ross: Dynamic Analysis of OAO Spacecraft
   Motion by Analog-Digital Simulation. 1962 IRE International Convention
   Record. Part V Aerospace and Navigational Electronics; Military Elec-
   tronics; Radio Frequency Interference; Space Electronics and Telemetry,
   vol. 10, 1962, pp. 282-296.

2. Showman, Robert D.; Doolin, Brian F.; and Sullivan, G. Michael: Simple
   Processors of Star Tracker Commands for Stabilizing an Inertially
   Oriented Satellite. NASA TN D-4490, 1968.

3. Meyer, George: On the Use of Euler's Theorem on Rotations for the
   Synthesis of Attitude Control Systems. NASA TN D-3643, 1966.

VACUUM CHAMBER STAR SIMULATOR

MOUNTING PLATFORM

SPHERICAL BEARING

GIMBAL ASSEMBLY

INERTIA CONES

AIR THRUSTERS
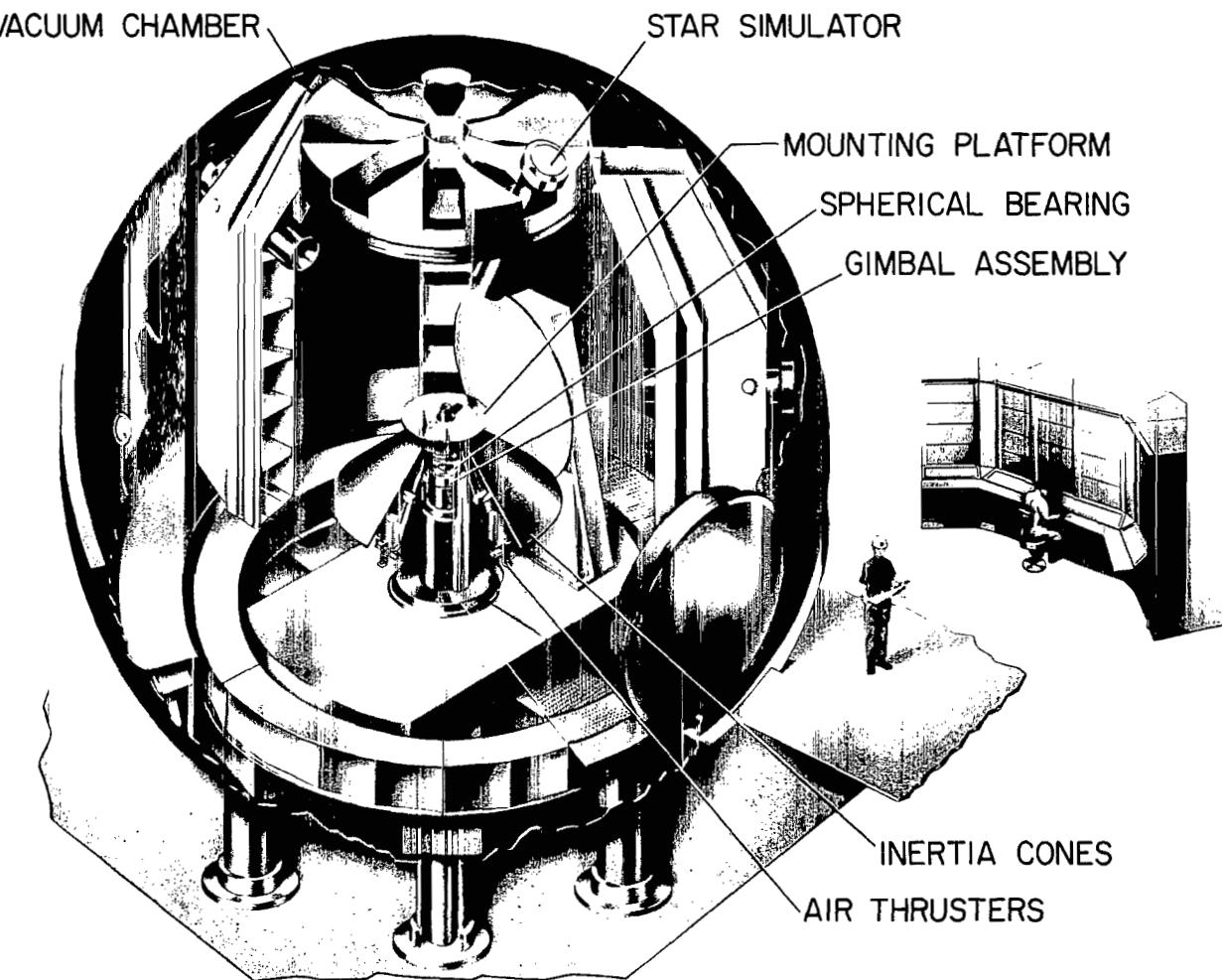
Figure 1.- Satellite attitude-control simulator.

STAR SIMULATOR

STAR TRACKER
No. 3
No. 2

RATE GYRO PACKAGE

REACTION WHEEL
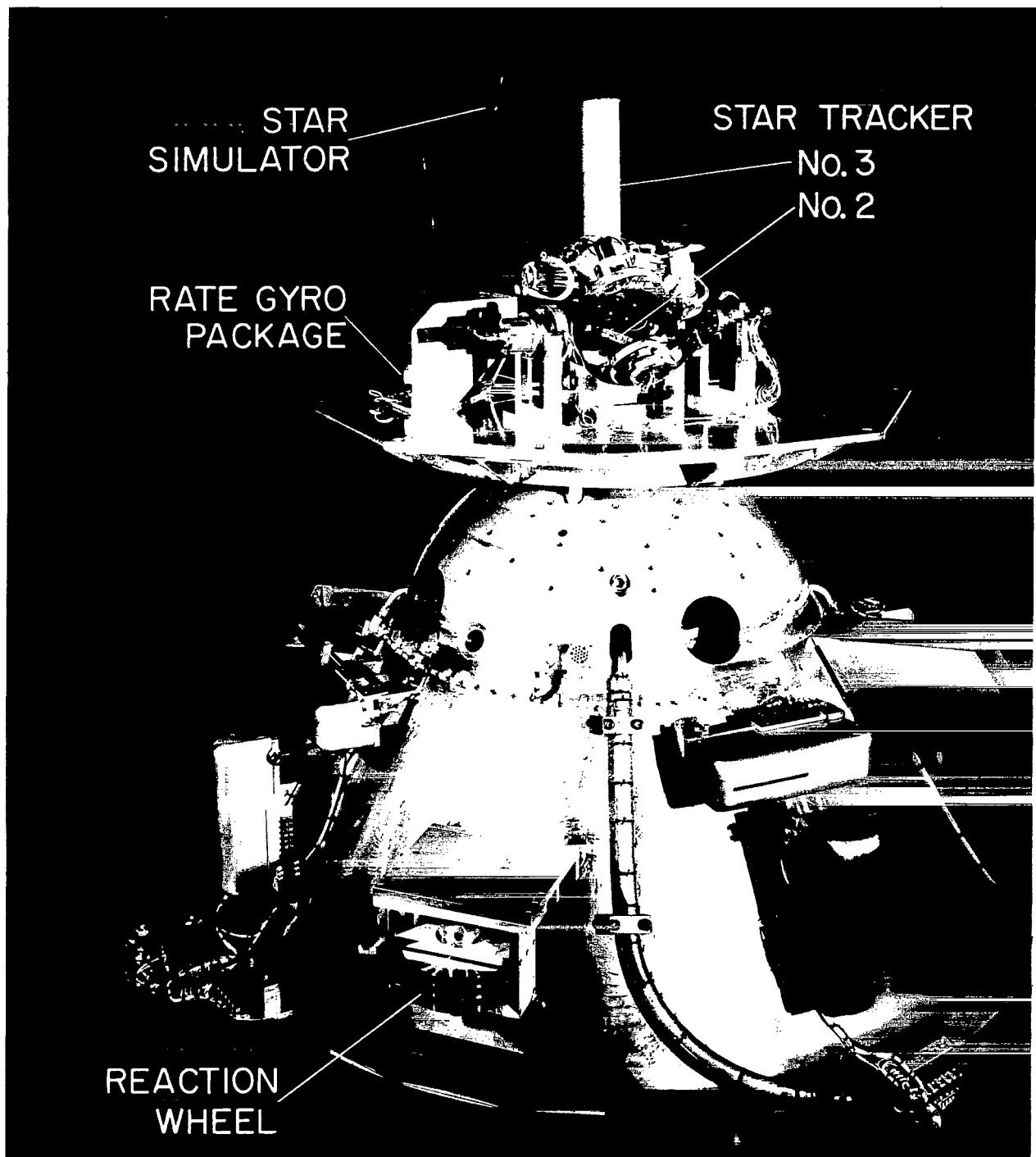
Figure 2.- Air bearing table with associated equipment.
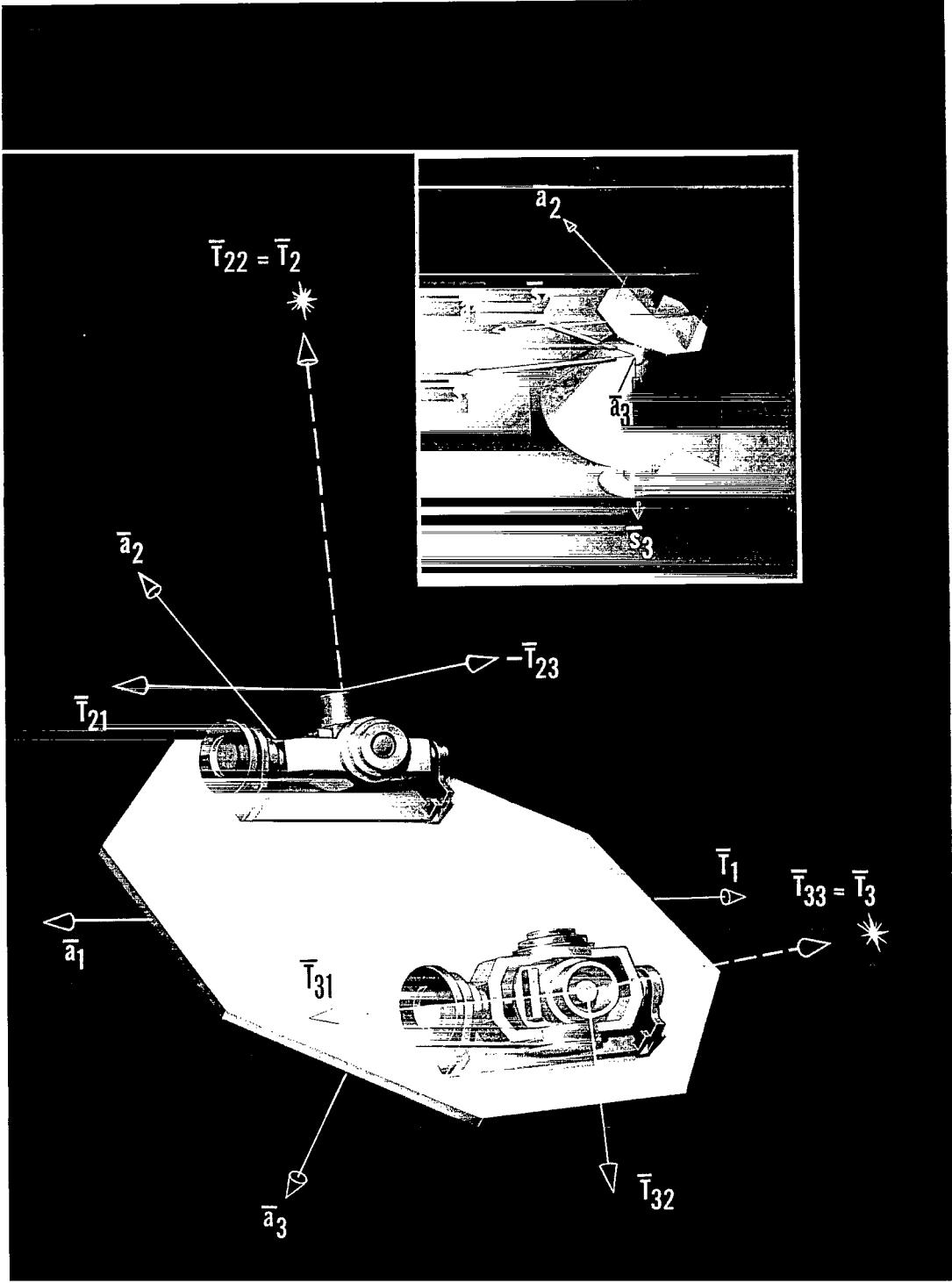
Figure 3.- Coordinate systems orientation.
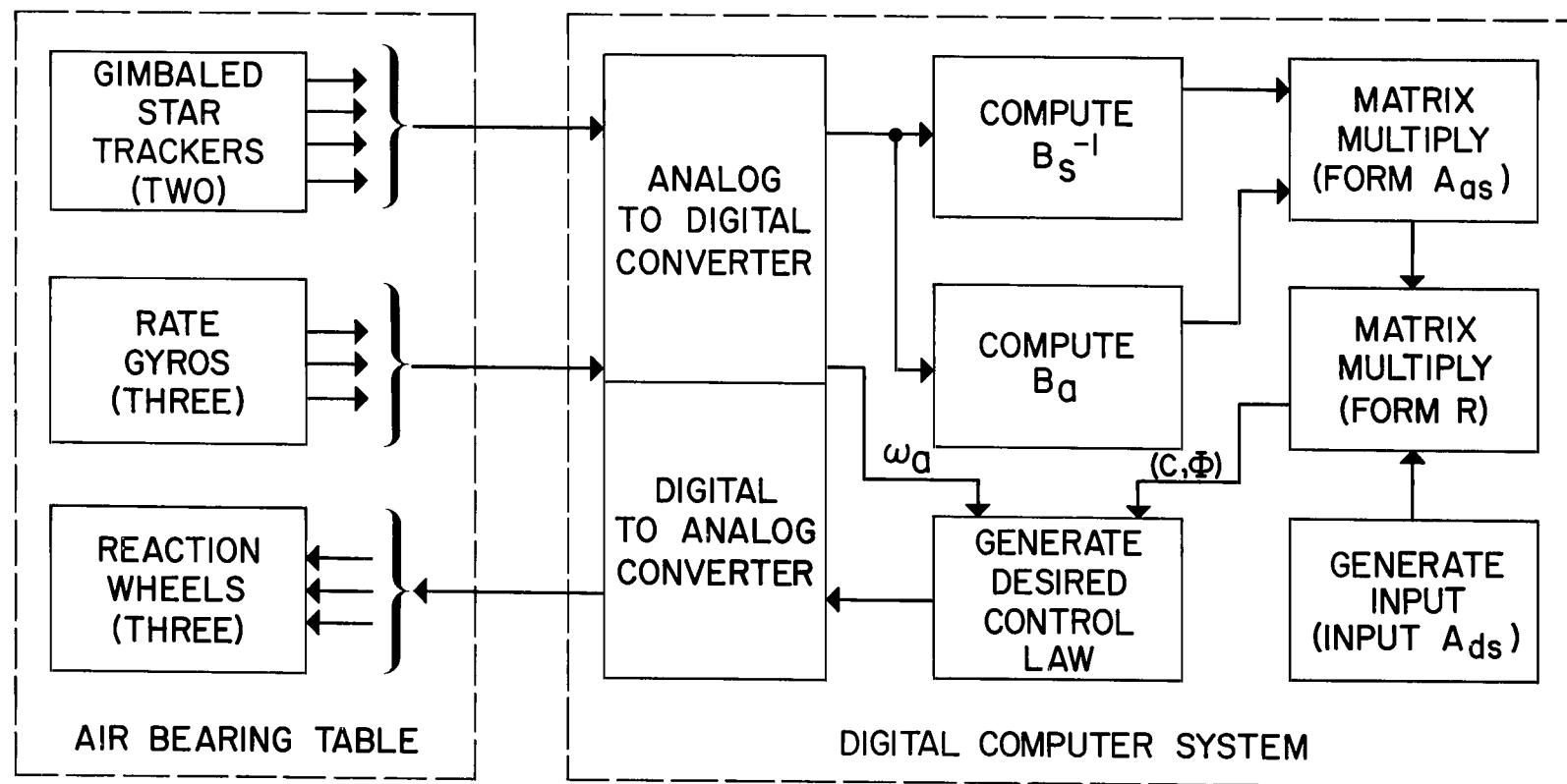
Figure 4.- Block diagram of the control system.

SYSTEM PERFORMANCE
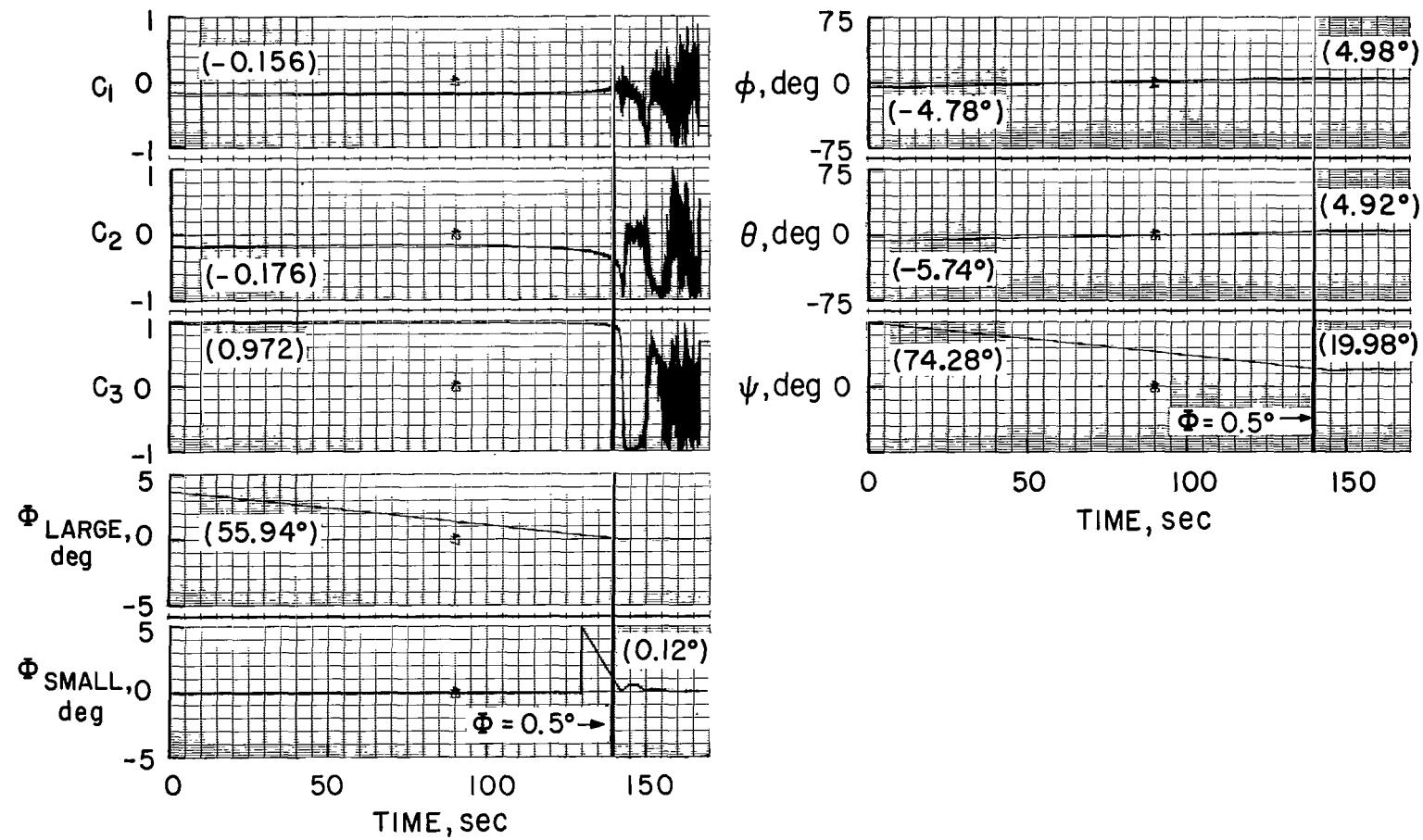
Figure 5.- Gyro rate damping - single command.
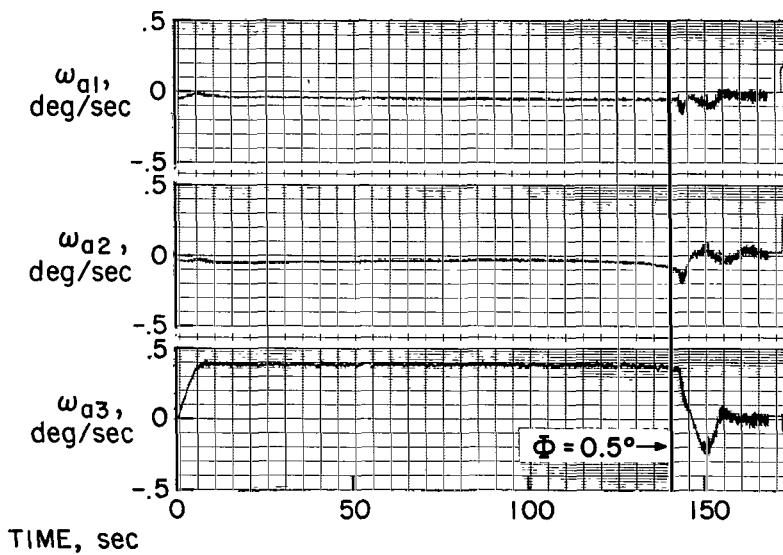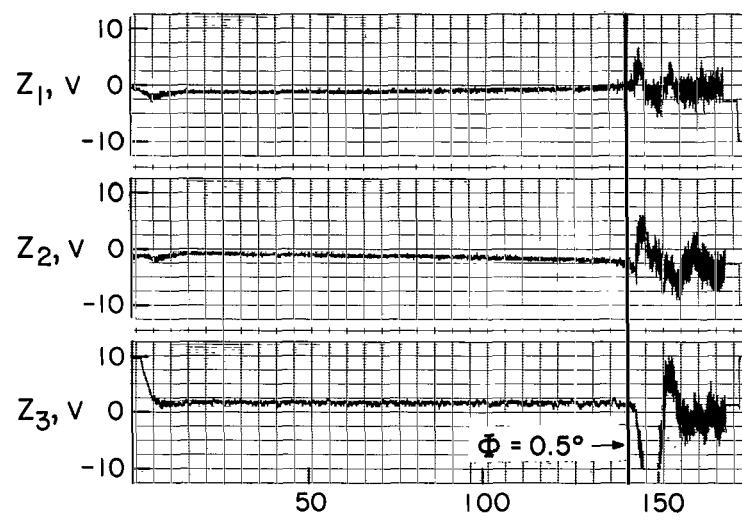
Figure 5.- Gyro rate damping - single command - Concluded.
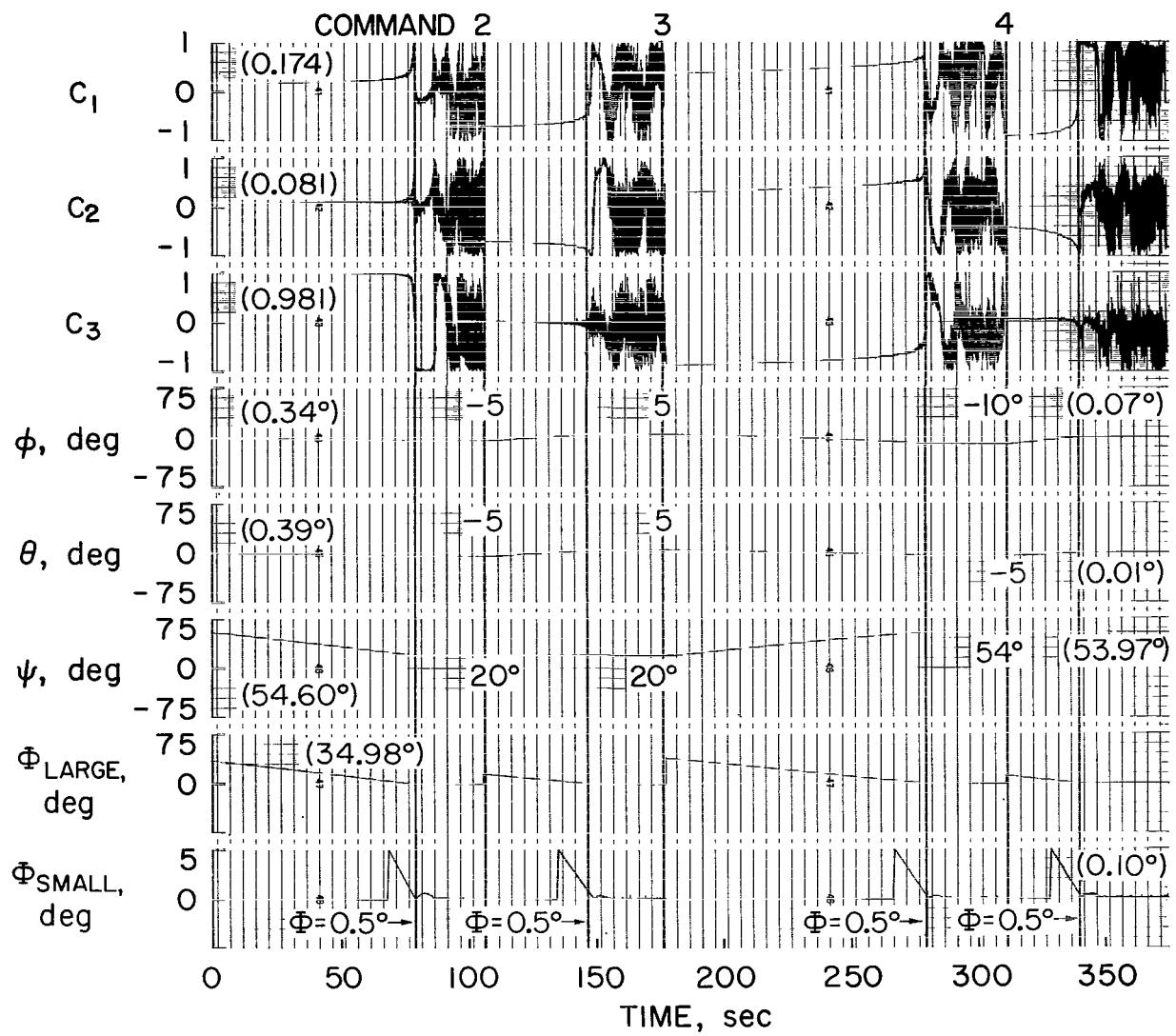
Figure 6.- Gyro rate damping - multiple command.
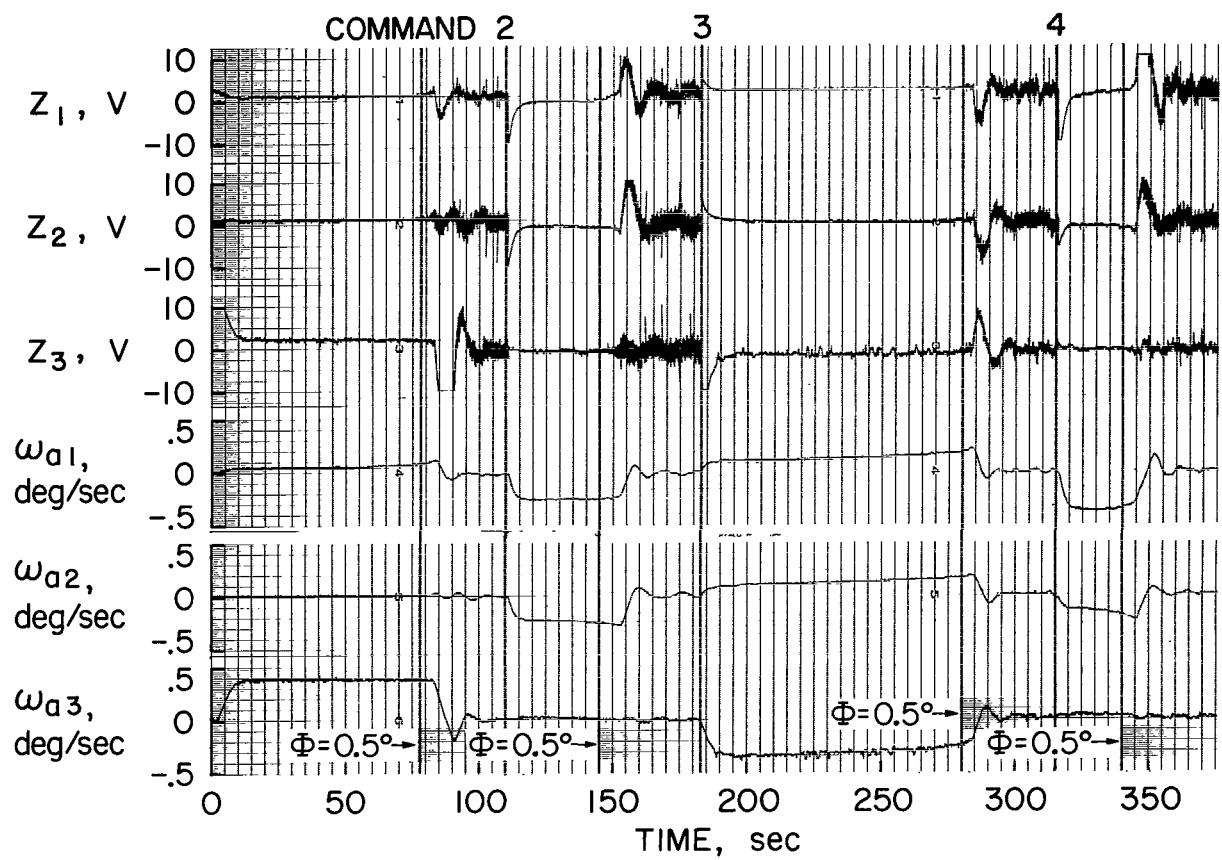
Figure 6.- Gyro rate damping - multiple command - Concluded.
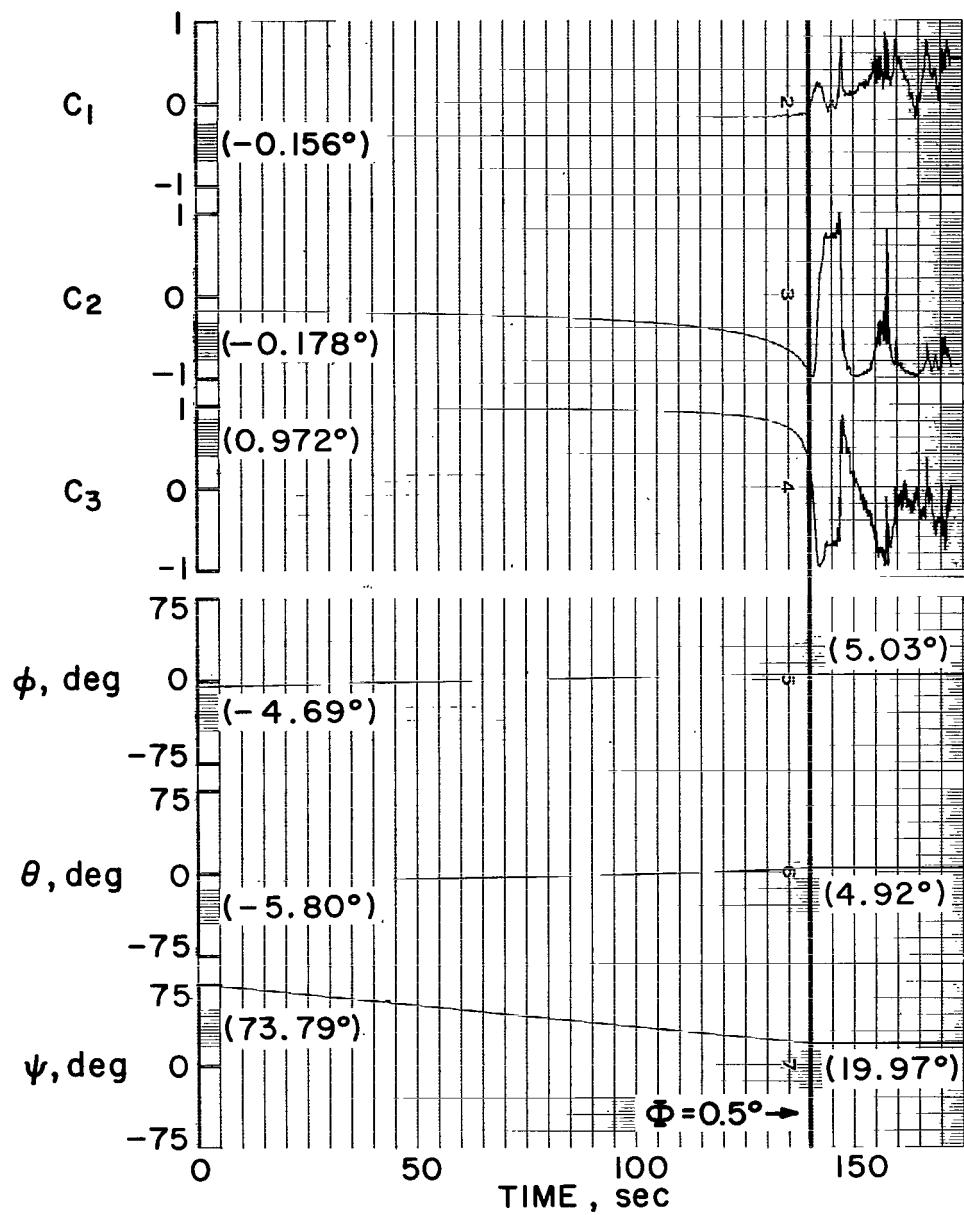
Figure 7.- Rate damping derived from A_{as} - single command.
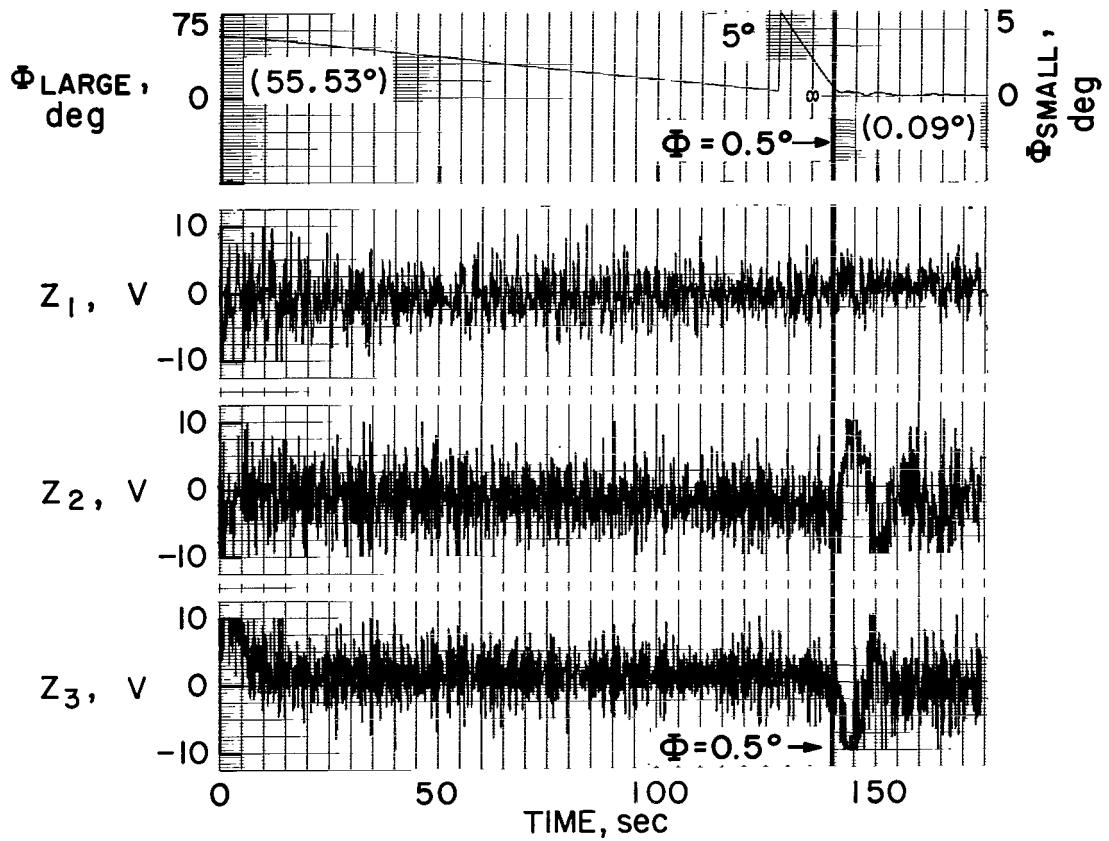
Figure 7.- Rate damping derived from A_{as} - single command - Continued.
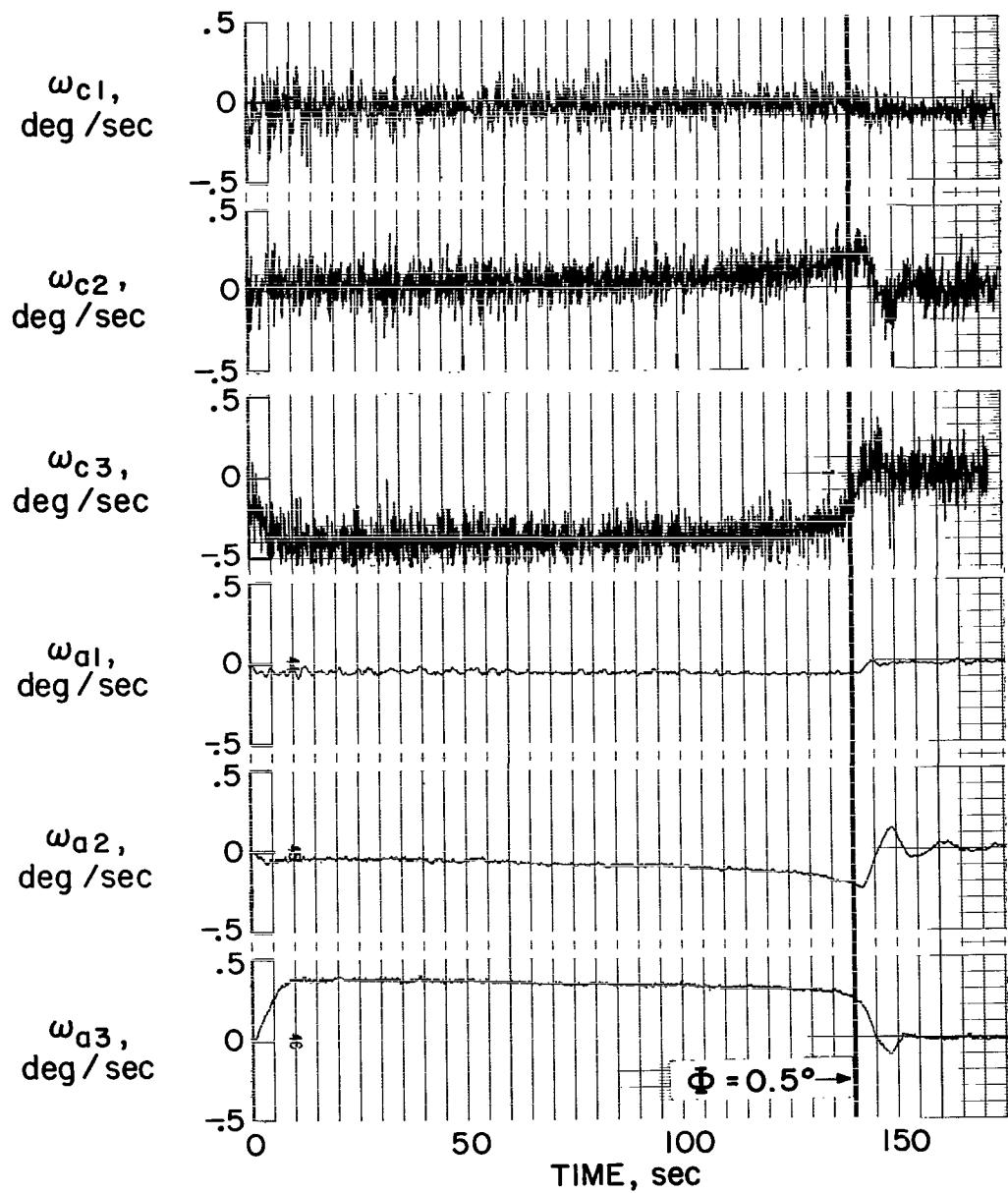
Figure 7.- Rate damping derived from A_{as} - single command - Concluded.
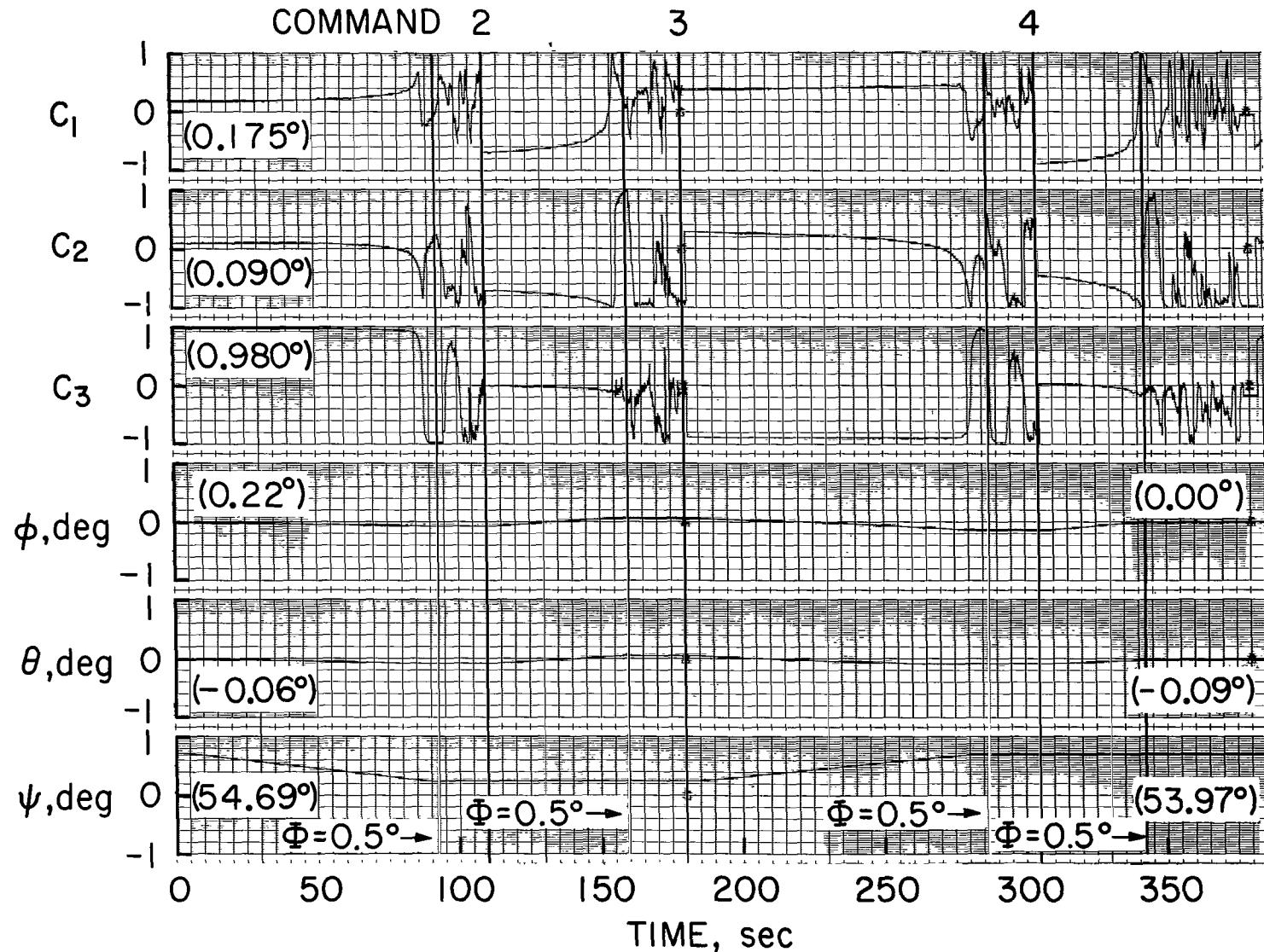
Figure 8.- Rate damping derived from A_{as} - multiple command.
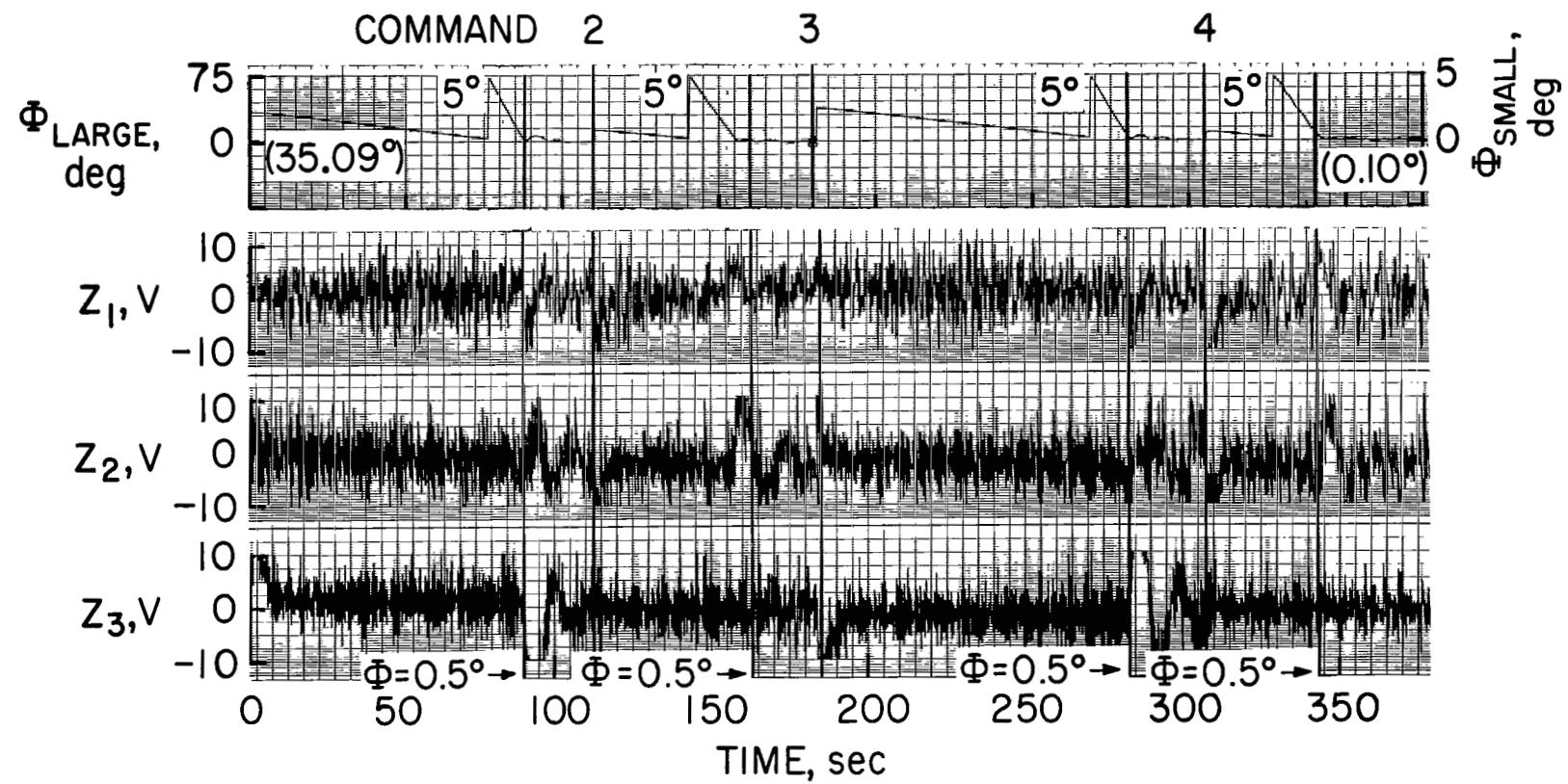
Figure 8.- Rate damping derived from A_{as} - multiple command - Continued.
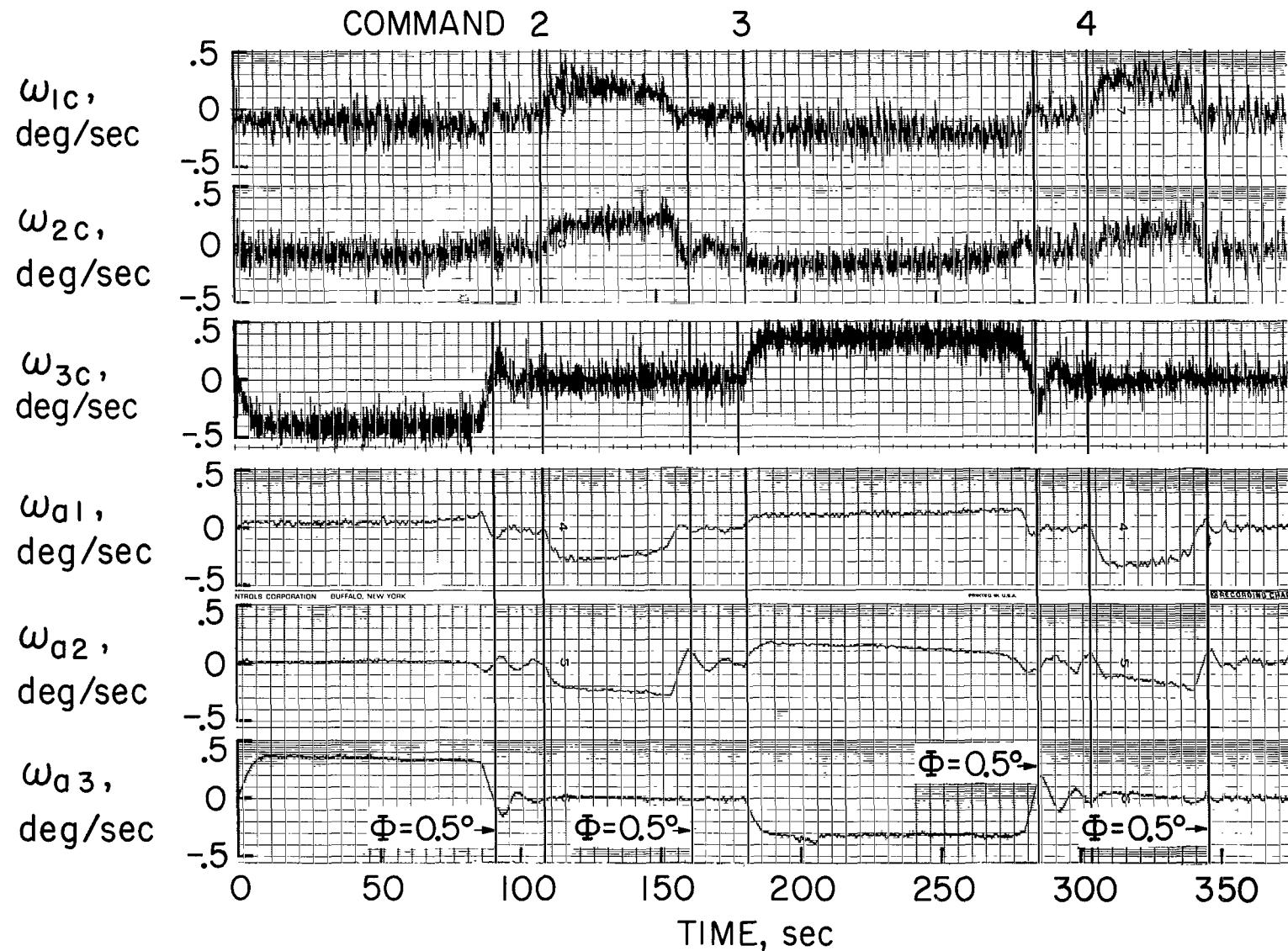
Figure 8.- Rate damping derived from A_{as} - multiple command - Concluded.
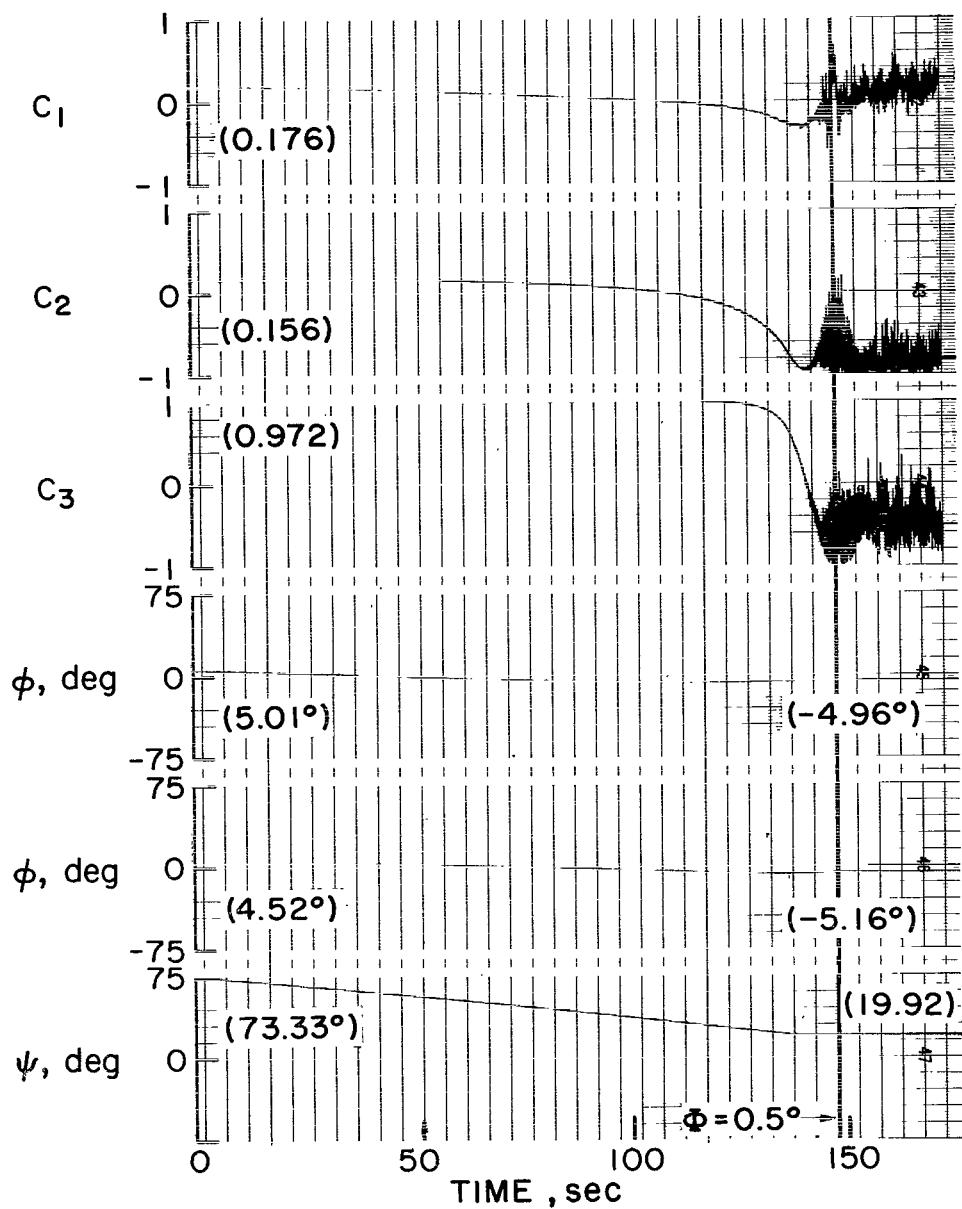
Figure 9.- Tachometer rate damping - single command.

Figure 9.- Tachometer rate damping - single command - Concluded.
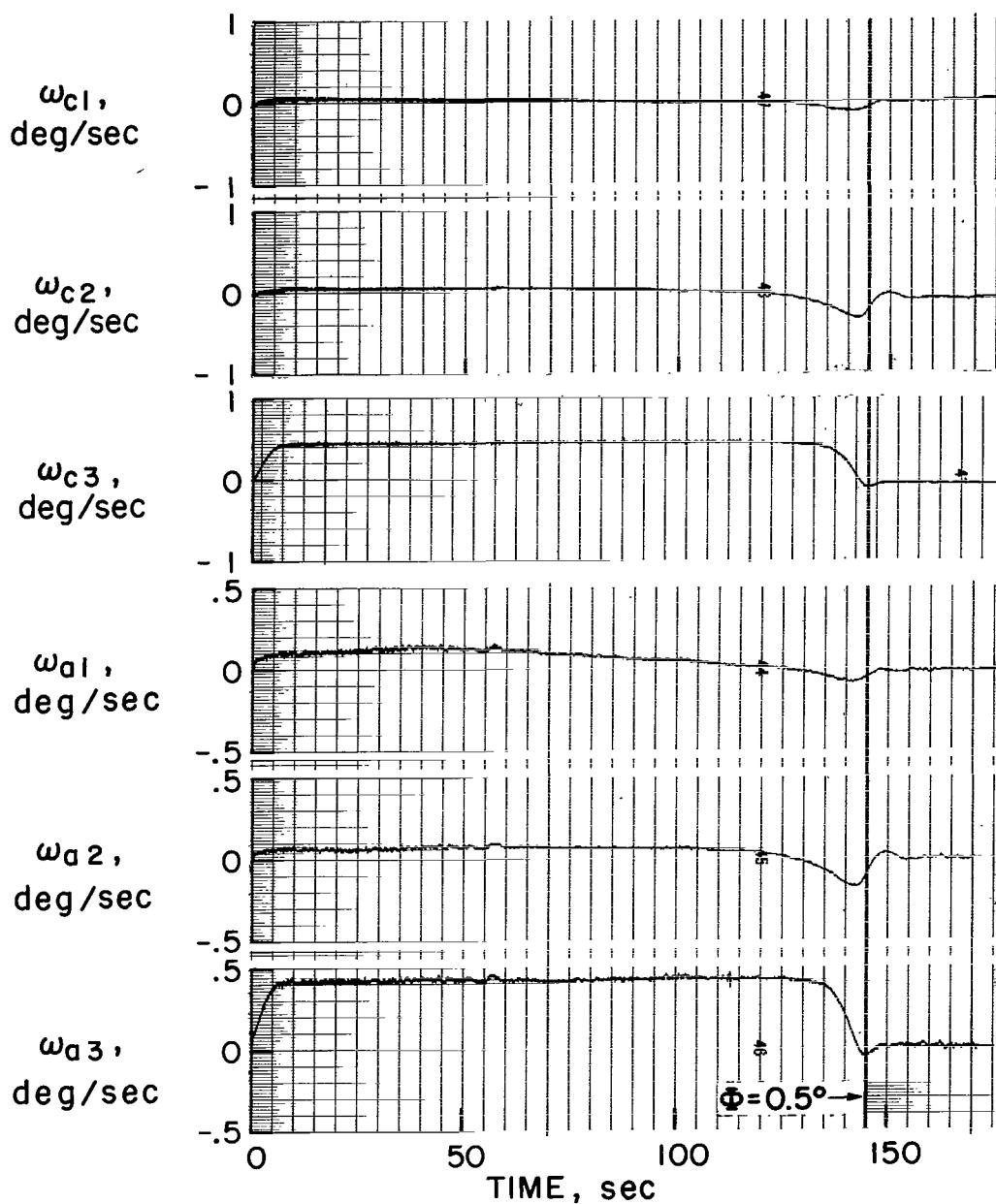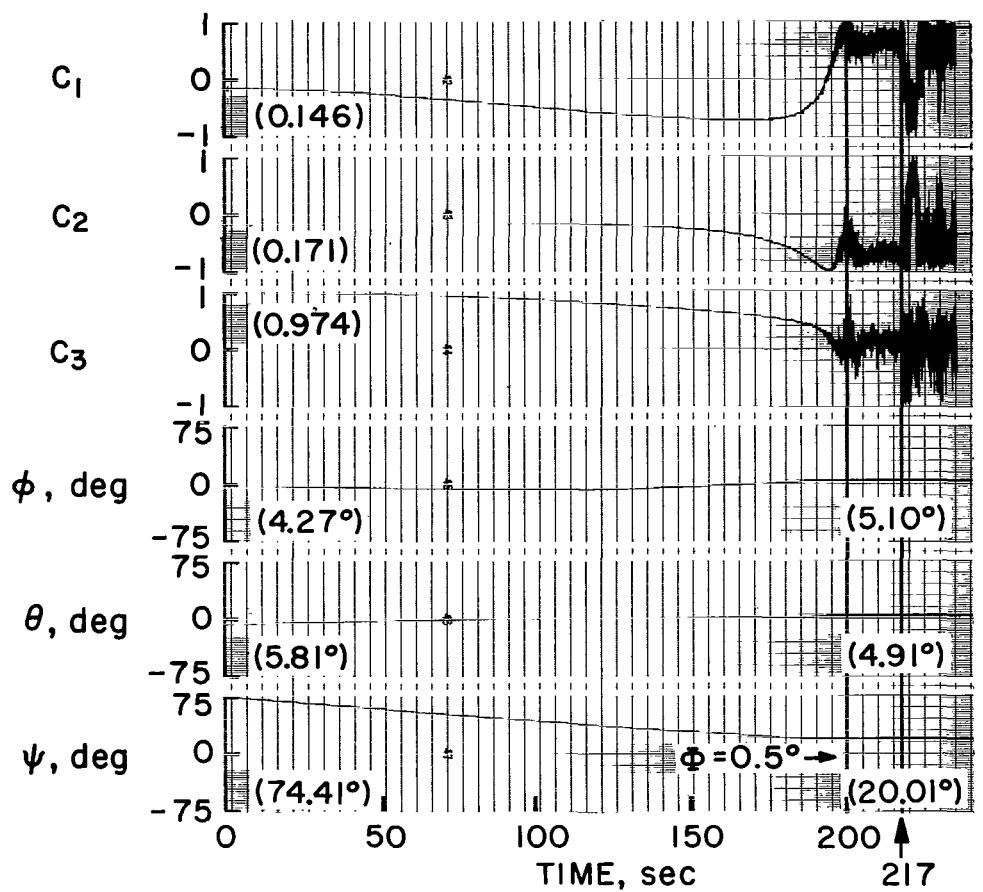
Figure 10.- Tachometer rate damping - momentum buildup compensation.
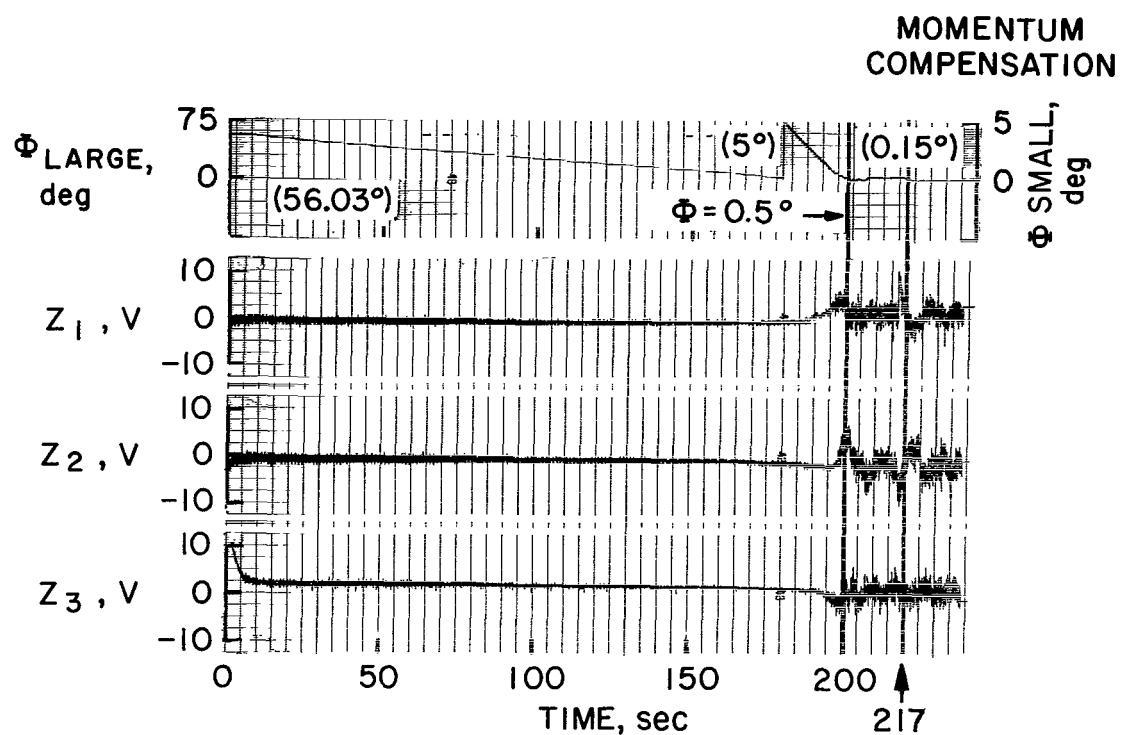
Figure 10.- Tachometer rate damping - momentum buildup compensation - Continued.
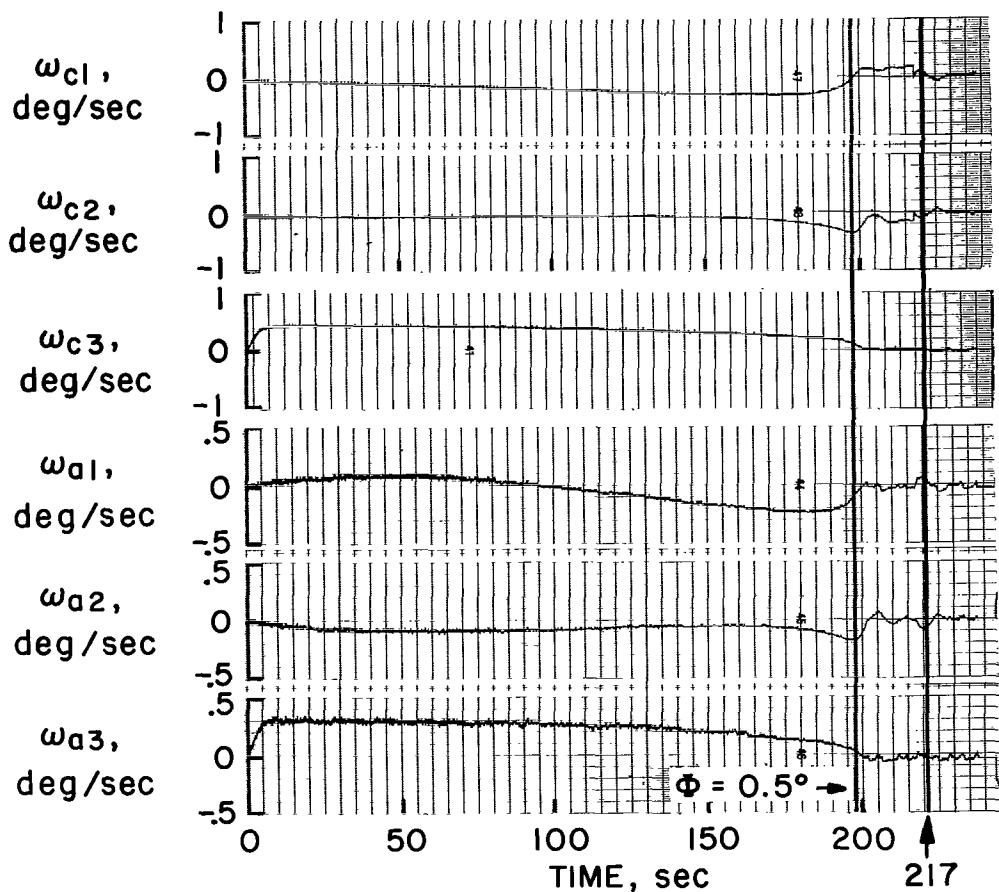
Figure 10.- Tachometer rate damping - momentum buildup compensation - Concluded.
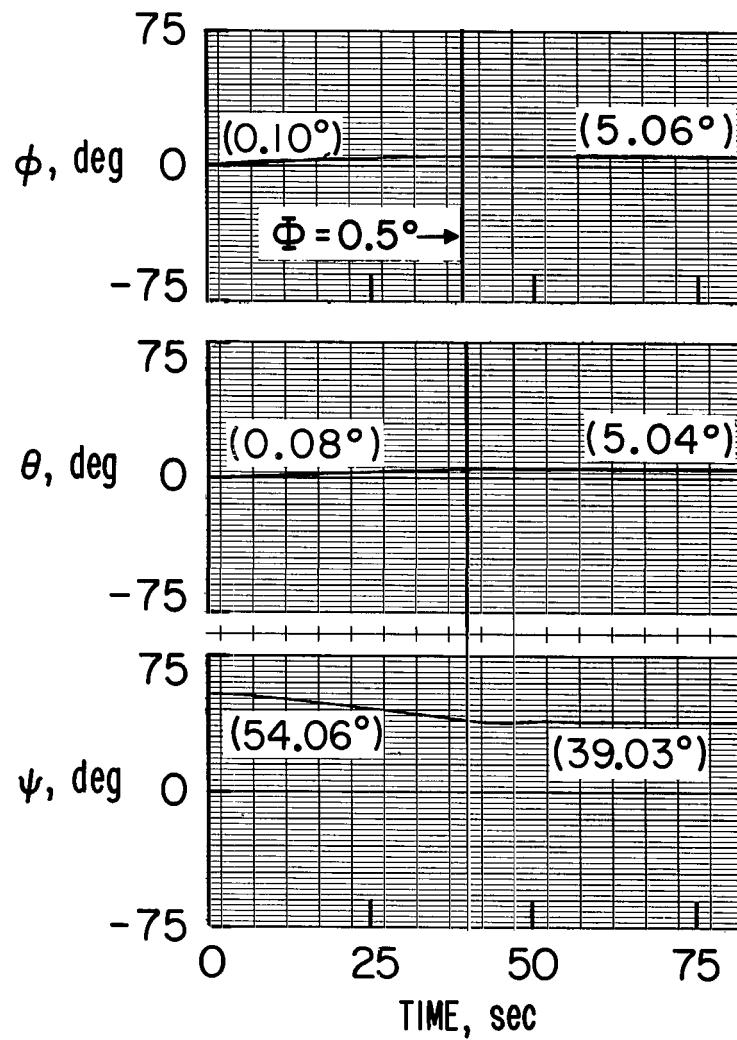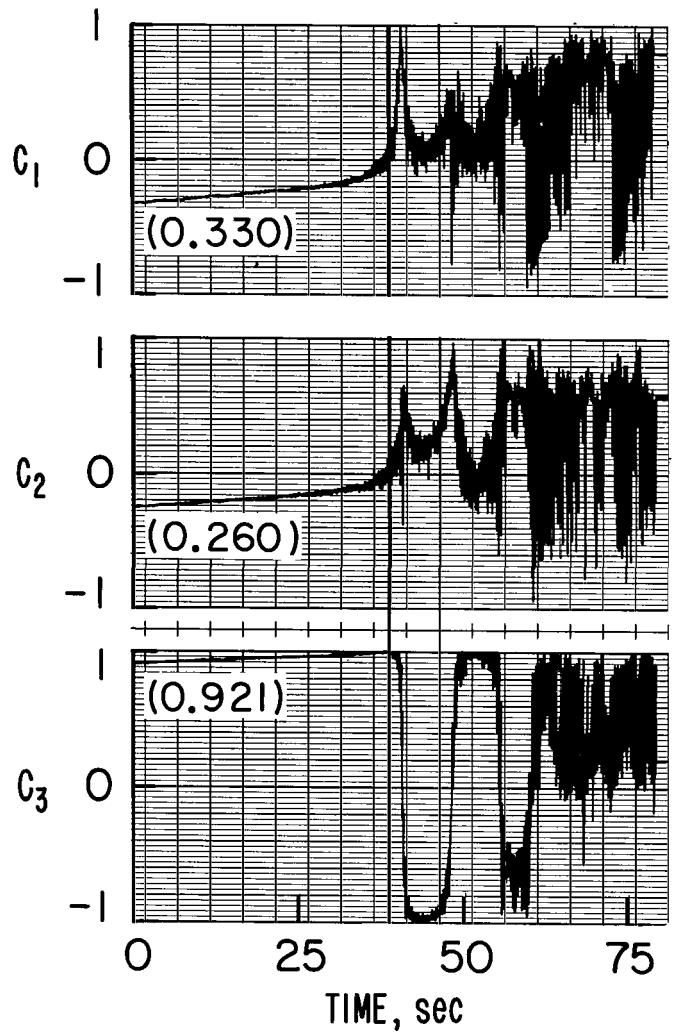
Figure 11.- Gyro system operating with initial momentum.
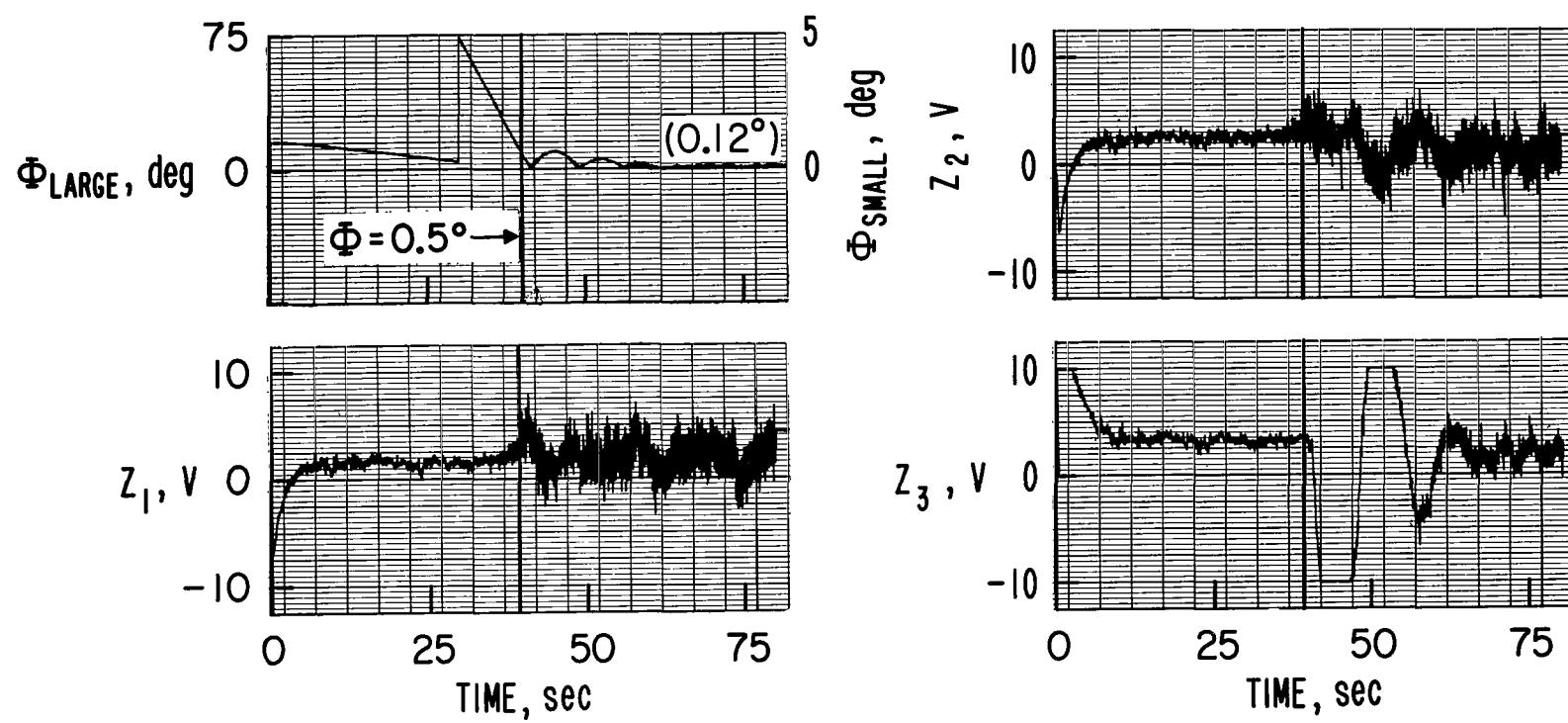
Figure 11.- Gyro system operating with initial momentum - Continued.
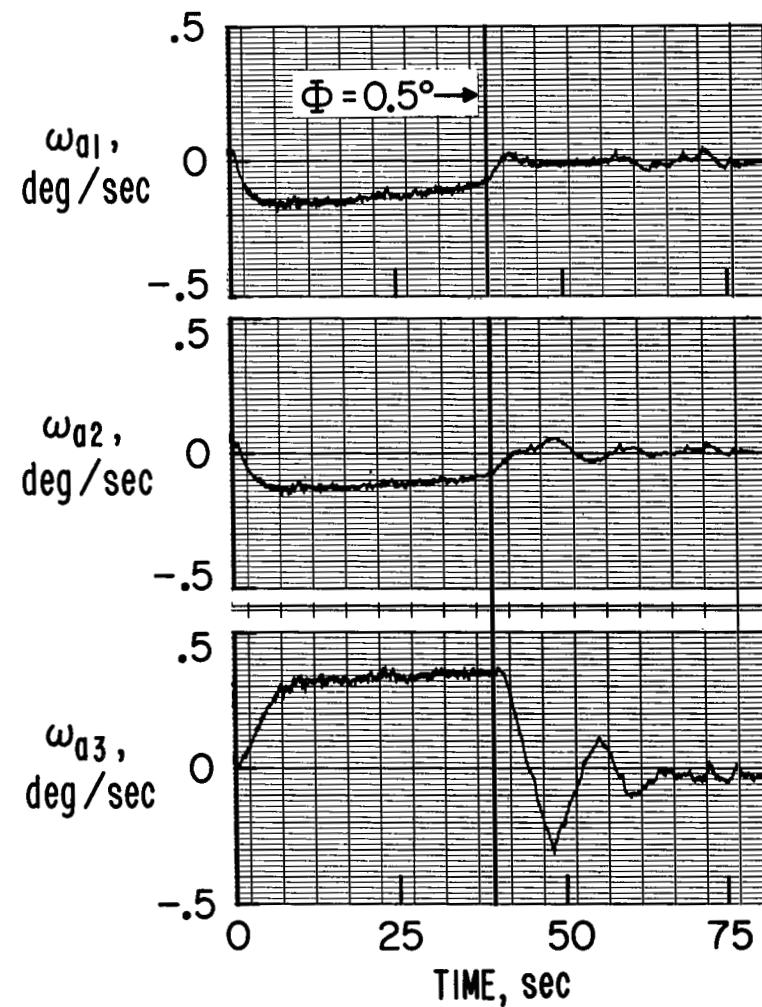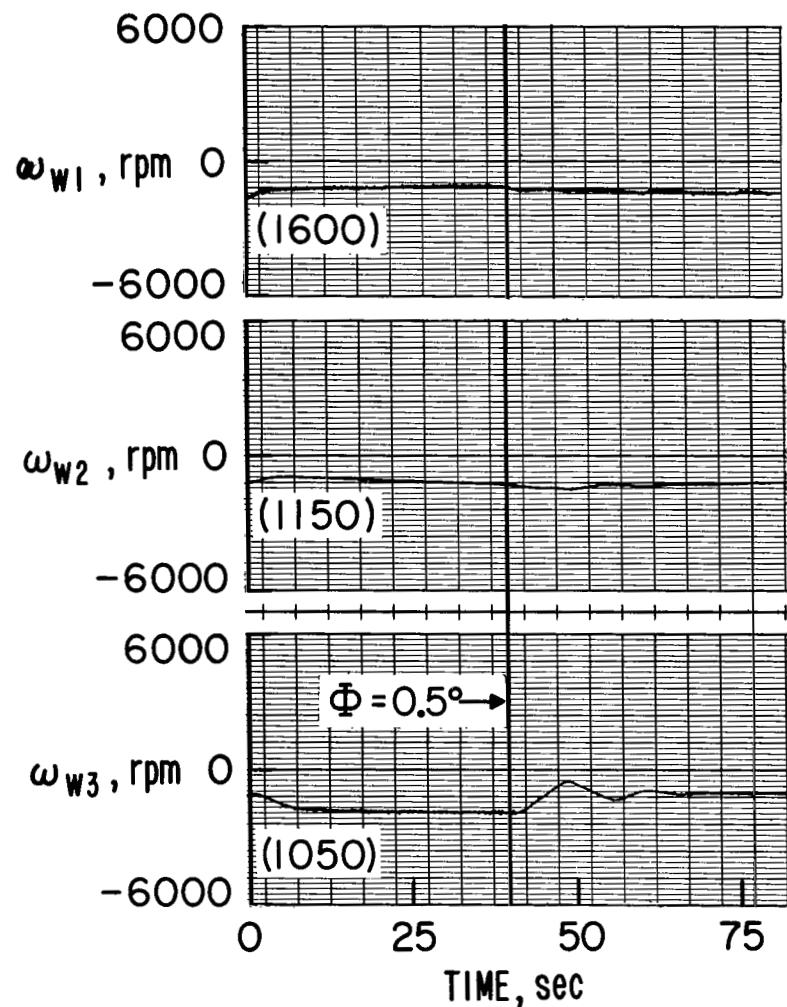
Figure 11.- Gyro system operating with initial momentum - Concluded.

FIRST CLASS MAIL

"The aeronautical and space activities of the United States shall be conducted so as to contribute . . . to the expansion of human knowledge of phenomena in the atmosphere and space. The Administration shall provide for the widest practicable and appropriate dissemination of information concerning its activities and the results thereof."

—NATIONAL AERONAUTICS AND SPACE ACT OF 1958

NASA SCIENTIFIC AND TECHNICAL PUBLICATIONS

TECHNICAL REPORTS: Scientific and technical information considered important, complete, and a lasting contribution to existing knowledge.

TECHNICAL NOTES: Information less broad in scope but nevertheless of importance as a contribution to existing knowledge.

TECHNICAL MEMORANDUMS: Information receiving limited distribution because of preliminary data, security classification, or other reasons.

CONTRACTOR REPORTS: Scientific and technical information generated under a NASA contract or grant and considered an important contribution to existing knowledge.

TECHNICAL TRANSLATIONS: Information published in a foreign language considered to merit NASA distribution in English.

SPECIAL PUBLICATIONS: Information derived from or of value to NASA activities. Publications include conference proceedings, monographs, data compilations, handbooks, sourcebooks, and special bibliographies.

TECHNOLOGY UTILIZATION PUBLICATIONS: Information on technology used by NASA that may be of particular interest in commercial and other non-aerospace applications. Publications include Tech Briefs, Technology Utilization Reports and Notes, and Technology Surveys.

Details on the availability of these publications may be obtained from:

SCIENTIFIC AND TECHNICAL INFORMATION DIVISION

NATIONAL AERONAUTICS AND SPACE ADMINISTRATION
Washington, D.C. 20546